

AD-A224 811

DTIC FILE COPY

SAIC 90/1163

2

**NETSIM: A COMPUTER PROGRAM FOR SIMULATING  
DETECTION AND LOCATION CAPABILITY  
OF REGIONAL SEISMIC NETWORKS**

Thomas J. Sereno, Jr.  
Steven R. Bratt  
Gaymond Yee

DTIC  
SELECTED  
JUL 31 1990  
S D  
D CS

Science Applications International Corporation  
10260 Campus Point Drive  
San Diego, California 92121

March 1990

Annual Technical Report  
1 January 1989 to 1 January 1990

The views and conclusions contained in this document are those of the authors and should not be interpreted as representing the official policies, either expressed or implied, of the Defense Advanced Research Projects Agency or the US Government.

**DISTRIBUTION STATEMENT A**

Approved for public release  
Distribution Unlimited

Sponsored By:

Defense Advanced Research Projects Agency (DARPA)  
Nuclear Monitoring Research Office (NMRO)  
Seismic Detection Capability Modeling

ARPA Order No. 4511 (Amendment 19)

Issued by AFTAC under Contract F08606-88-C-0033.

90 07 30 180

SAIC 90/1163

**NETSIM: A COMPUTER PROGRAM FOR SIMULATING  
DETECTION AND LOCATION CAPABILITY  
OF REGIONAL SEISMIC NETWORKS**

Thomas J. Sereno, Jr.  
Steven R. Bratt  
Gaymond Yee

Science Applications International Corporation  
10260 Campus Point Drive  
San Diego, California 92121



March 1990

Annual Technical Report  
1 January 1989 to 1 January 1990

The views and conclusions contained in this document are those of the authors and should not be interpreted as representing the official policies, either expressed or implied, of the Defense Advanced Research Projects Agency or the US Government.

Accession For	
NTIS CRA&I	<input checked="" type="checkbox"/>
DTIC TAB	<input type="checkbox"/>
Unannounced	<input type="checkbox"/>
Justification .....	
By .....	
Distribution /	
Availability Codes	
Dist	Avail and/or Special
A-1	

Sponsored By:

Defense Advanced Research Projects Agency (DARPA)  
Nuclear Monitoring Research Office (NMRO)  
Seismic Detection Capability Modeling

ARPA Order No. 4511 (Amendment 19)

Issued by AFTAC under Contract F08606-88-C-0033.

REPORT DOCUMENTATION PAGE

1a. REPORT SECURITY CLASSIFICATION Unclassified		1b. RESTRICTIVE MARKINGS	
2a. SECURITY CLASSIFICATION AUTHORITY		3. DISTRIBUTION/AVAILABILITY OF REPORT Approved for Public Release, distribution unlimited	
2b. DECLASSIFICATION/DOWNGRADING SCHEDULE			
4. PERFORMING ORGANIZATION REPORT NUMBER(S) SAIC-90/1163		5. MONITORING ORGANIZATION REPORT NUMBER(S)	
6a. NAME OF PERFORMING ORGANIZATION Science Applications International Corporation	6b. OFFICE SYMBOL (if applicable)	7a. NAME OF MONITORING ORGANIZATION Air Force Technical Applications Center/TTR	
6c. ADDRESS (City, State, and ZIP Code) 10260 Campus Pt. Drive San Diego CA 92121		7b. ADDRESS (City, State, and ZIP Code) HQ/AFTAC/TTR Patrick Air Force Base, FL 32925-6001	
8a. NAME OF FUNDING/SPONSORING ORGANIZATION Defense Advanced Research Projects Agency	8b. OFFICE SYMBOL (if applicable) DARPA	9. PROCUREMENT INSTRUMENT IDENTIFICATION NUMBER F08606-88-C-0033	
8c. ADDRESS (City, State, and ZIP Code) 1400 Wilson Blvd Arlington VA 22209		10. SOURCE OF FUNDING NUMBERS	
		PROGRAM ELEMENT NO. 62714E	PROJECT NO. 8A10
		TASK NO. SOW 3.1	WORK UNIT ACCESSION NO.
11. TITLE (Include Security Classification) NETSIM: A Computer Program for Simulating Detection and Location Capability of Regional Seismic Networks			
12. PERSONAL AUTHOR(S) Thomas J. Sereno, Jr., Steven R. Bratt, Gaymond Yee			
13a. TYPE OF REPORT Annual Report No. 1	13b. TIME COVERED FROM 1/1/89 TO 12/31/89	14. DATE OF REPORT (Year, Month, Day) 1990 March	15. PAGE COUNT 98
16. SUPPLEMENTARY NOTATION <i>cont'd from back</i>			
17. COSATI CODES		18. SUBJECT TERMS (Continue on reverse if necessary and identify by block number)	
FIELD 8	GROUP 11	COMPUTER PROGRAMS; MODULES (ELECTRONICS); Treaty Monitoring, Verification, Networks Simulation; Detection Capability, Location Capability <i>input/output data</i> ; COMPUTER PROGRAM VERIFICATION; SEISMIC DATA.	
19. ABSTRACT (Continue on reverse if necessary and identify by block number)			
<p>This report describes a computer program called <i>NetSim</i> that calculates simulations of detection and location capability of seismic networks that include regional stations and arrays. These simulations are used to assess seismic network capability to monitor existing and proposed nuclear explosion test limitation treaties. The main advantage of <i>NetSim</i> compared to similar computer programs (e.g., <i>NETWORTH</i> and <i>SNAP/D</i>) is the incorporation of frequency dependence in the source model, noise estimates (for both primary and secondary phases), attenuation estimates, and array gain estimates. This is important for simulating the monitoring capability of regional networks, since the dominant signal frequency of regional phases often varies substantially with epicentral distance. The report provides functional descriptions of the <i>NetSim</i> detection and location modules and sample runs for frequency-independent and frequency-dependent input</p>			
20. DISTRIBUTION/AVAILABILITY OF ABSTRACT <input type="checkbox"/> UNCLASSIFIED/UNLIMITED <input checked="" type="checkbox"/> SAME AS RPT. <input type="checkbox"/> DTIC USERS		21. ABSTRACT SECURITY CLASSIFICATION Unclassified	
22a. NAME OF RESPONSIBLE INDIVIDUAL Dr. Dean Clauter		22b. TELEPHONE (Include Area Code) (407) 494-5263	22c. OFFICE SYMBOL AFTAC/TTR

CONFID.

IS ALSO INVESTIGATED.

parameters. We also investigate the accuracy of location uncertainties computed using two methods that attempt to account for the effect of undetected phases. These are the probability-weighted approach used in SNAP/D and a Monte Carlo approach that mimics the way location uncertainties vary in practice. Keywords: Block 18 on front

Unclassified

## Table of Contents

<b>LIST OF FIGURES</b> .....	v
<b>LIST OF TABLES</b> .....	vii
<b>1. INTRODUCTION</b> .....	1
1.1 Project Objectives .....	1
1.2 Current Status .....	1
1.3 Outline of the Report .....	2
<b>2. NETSIM OVERVIEW</b> .....	3
2.1 Introduction .....	3
2.2 Detection Module .....	3
2.2.1 <i>Signal</i> .....	4
2.2.2 <i>Noise</i> .....	7
2.3 Location Module .....	8
2.3.1 <i>Probability Weighting</i> .....	9
2.3.2 <i>Monte Carlo</i> .....	9
<b>3. NETSIM INPUT/OUTPUT</b> .....	11
3.1 Input Data .....	11
3.2 Output Data .....	14
3.3 Graphics .....	15
<b>4. SAMPLE RUNS</b> .....	17
4.1 Frequency-Independent Input .....	17
4.2 Frequency-Dependent Input .....	49
4.3 Probability-Weighted and Monte Carlo Location .....	49
<b>5. SUMMARY</b> .....	59
<b>ACKNOWLEDGMENTS</b> .....	61
<b>REFERENCES</b> .....	63

**APPENDIX A: INPUT/OUTPUT DATA TABLES ..... 65**

**DISTRIBUTION LIST ..... 91**

## LIST OF FIGURES

	Page
<b>Figure 3.1.</b> Schematic top-level data flow diagram for <i>NetSim</i> .	12
<b>Figure 4.1.</b> Input source spectra as a function of scalar seismic moment, $M_0$ . Each curve is labeled by $\log M_0$ . The corner frequency scales inversely with the cube root of the long-period level. The source scaling is from <i>Sereno et al.</i> [1988]. These spectra are stored in a two-dimensional data table called <i>expl.sor</i> (Table 4.2).	21
<b>Figure 4.2.</b> Input <i>P</i> -wave attenuation curves as a function of frequency. These curves are based on attenuation along paths to the NORESS array [ <i>Sereno et al.</i> , 1988]. These $B(\Delta, f)$ are stored in a two-dimensional data table called <i>pstable.atn</i> (Table 4.3).	24
<b>Figure 4.3.</b> Location of seismic stations comprising the hypothetical network used in our detection and location capability simulations. The station coordinates are stored in the station file, <i>a20x13.sta</i> (Table 4.4).	26
<b>Figure 4.4.</b> Input local site response for array stations. Only the array gain portion of the site response is included. We assume a linear decrease in beam gain from $\sqrt{N}$ at 1 Hz to 1.0 at 20 Hz [ <i>Sereno et al.</i> , 1988]. The site response as a function of frequency is stored in a one-dimensional data table called <i>array.srs</i> (Table 4.4).	28
<b>Figure 4.5.</b> Input ambient noise power spectral density. The same ambient noise spectrum is assumed for all stations in the network. This is the average single-channel noise spectrum at NORESS [ <i>Suteau-Henson and Bache</i> , 1988]. The ambient noise is stored in a one-dimensional data table called <i>ambient.noi</i> (Table 4.5).	30
<b>Figure 4.6.</b> Contours of the 90% <i>MLg</i> thresholds for detecting 3 <i>P</i> phases at (a) 1 Hz, and (b) 10 Hz.	50
<b>Figure 4.7.</b> Contours of the 90% <i>MLg</i> thresholds for detecting 3 <i>P</i> phases using broad band (1–20 Hz) input.	52
<b>Figure 4.8.</b> Frequency of the maximum SNR as a function of epicentral distance for <i>P</i> phases. This figure plots the values in Table 4.9 for an epicenter in the western USSR (60° N, 60° E).	53

**Figure 4.9.** Contours of the semi-major axis (SMA, in kilometers) computed using the probability-weighted approach for events at the 3 *P* detection threshold. Uncertainties are given at the 90% confidence level. Depth is constrained to the surface. 56

**Figure 4.10.** Contours of the SMA computed using the Monte Carlo approach for events at the 3 *P* detection threshold. (a) Median realization and (b) 90th percentile realization. Uncertainties are given at the 90% confidence level. Depth is constrained to the surface. 57

**Figure 4.11.** Histogram of location uncertainties (SMA) determined from 100 Monte Carlo realizations of location solutions in the western Soviet Union (60° N, 60° E). The probability-weighted (PW), the median Monte Carlo realization (MC50), and the 90th percentile Monte Carlo realization (MC90) SMA values are marked. The fraction of Monte Carlo realizations with enough data to constrain the epicenter is also listed. Event magnitudes are (a) *MLg* 3.0, (b) *MLg* 2.58 (3 *P* detection threshold), and (c) *MLg* 2.23 (2 *P* detection threshold). 58

## LIST OF TABLES

	Page
Table 4.1. Sample control data.	19
Table 4.2. Sample source data.	20
Table 4.3. Sample propagation data.	22
Table 4.4. Sample site/station data.	25
Table 4.5. Sample noise data.	29
Table 4.6. Sample output graphics file.	39
Table 4.7. Sample output list file.	42
Table 4.8. Sample control file (frequency-dependent input).	51
Table 4.9. Sample list file (frequency-dependent input).	54
Table 5.1. The 90% <i>MLg</i> thresholds for a network of 33 stations.	59
Table A.1. Control file.	66
Table A.2. Epicenter file.	69
Table A.3. Source media file.	70
Table A.4. Source grid file.	71
Table A.5. Source spectra file.	72
Table A.6. Path media file.	74
Table A.7. Path grid file.	75
Table A.8. Attenuation file.	76
Table A.9. Travel time file.	77
Table A.10. Station file.	80
Table A.11. Site Response file.	81

<b>Table A.12. Ambient noise file.</b>	83
<b>Table A.13. Noise factor file.</b>	84
<b>Table A.14. Graphics file.</b>	86
<b>Table A.15. List file.</b>	87

## 1. INTRODUCTION

### 1.1 Project Objectives

The objective of this two-year study is to simulate detection and location capability of seismic networks including regional stations and arrays in and around the Soviet Union. Three specific research tasks are:

- (1) Enhance and validate the extended version of the Seismic Network Assessment Program for Detection [*SNAP/D*, Ciervo *et al.*, 1985] called *SNAP/DX* [Bratt *et al.*, 1987a] to accurately represent the treaty monitoring capability of seismic networks including regional stations and arrays.
- (2) Normalize *SNAP/DX* to the observed performance of existing stations and expected conditions in and around the Soviet Union.
- (3) Apply the normalized simulation methods to assess the treaty monitoring capability of existing and proposed seismic networks.

### 1.2 Current Status

The effort during the first year of this project was divided among *SNAP/DX* enhancement and *SNAP/DX* normalization. The first semi-annual report described the normalization results obtained during the first six months of the project [Serenio, 1989]. This included two studies: (1) a theoretical study of the sensitivity of *Pn* geometric spreading to the velocity gradient in the upper mantle, and (2) an empirical study of the attenuation of *Pn* and *Lg* phases recorded in eastern Kazakhstan. We have continued to work on the normalization since this first report, but the more recent work has been primarily in assembling a data base of regional events recorded by the NORESS and ARCESS arrays in Norway. We have processed data from nearly 100 events recorded by the two arrays. This processing includes interactive picking of regional phases, calculation of Fourier signal and noise spectra, and the determination of phase velocity, azimuth, amplitude, and dominant frequency. These signal spectra will be inverted for source and attenuation parameters near the beginning of the second year of the contract, and these results (along with the rest of the normalization results) will be included in the third semi-annual report for this project.

This annual report describes our enhancements to the *SNAP/DX* computer program. The most important of these enhancements is the introduction of frequency dependence into the estimates for the source, station noise (for primary and secondary phases), attenuation, and array gain. *SNAP/D* and *SNAP/DX* calculate detection and location capability at fixed frequency. This is adequate to represent the capability of teleseismic networks because the dominant signal frequency is only weakly dependent on distance. However, at regional distances the frequency of the maximum signal-to-noise ratio (SNR) may be strongly distance-dependent. Therefore, the detection capa-

bilities at individual stations in the network must be evaluated at a frequency that depends on epicentral distance.

### 1.3 Outline of the Report

This report is divided into five sections including this introduction. Section 2 is an overview of our new network simulation computer program, *NetSim*. We start with a brief introduction that describes the relationship between *NetSim* and other computer programs that have previously been used to assess the capability of seismic networks to monitor underground nuclear explosion testing. Next, we give functional descriptions of the *NetSim* detection and location modules. Section 3 summarizes the *NetSim* input and output data and graphics (Appendix A gives a detailed listing and description of each input and output parameter). Section 4 gives sample *NetSim* runs for frequency-dependent and frequency-independent input. Section 5 summarizes the main conclusions.

## 2. NETSIM OVERVIEW

### 2.1 Introduction

*NetSim* is a computer program to simulate the detection and location capability of seismic networks including regional stations and arrays. The main advantage of *NetSim* compared to similar computer programs is the incorporation of frequency dependence in the estimates for the source, station noise, attenuation, and array gain. Computer programs that simulate network performance at fixed frequency include *NETWORTH* [Wirth, 1977], *SNAP/D* [Ciervo et al., 1985], and an extended version of *SNAP/D* called *SNAP/DX* [Bratt et al., 1987a]. *SNAP/D* allows specification of multiwave detection criteria; a feature that is not available in its predecessor, *NETWORTH*. *SNAP/DX* uses the same detection module as *SNAP/D*, but it has a new location module. This new module is based on the *TTAZLOC* location program of Bratt and Bache [1988], and uses estimates of both arrival time and azimuth standard deviation to estimate the location uncertainty. *SNAP/DX* offers two approaches for approximating the effect of undetected phases on the location uncertainties; the *probability-weighted* approach used in *SNAP/D*, and a *Monte Carlo* approach that mimics the way location uncertainties vary in practice. *NetSim* uses the enhanced *SNAP/DX* location module combined with an enhanced detection module that incorporates frequency dependence in the propagation and noise characteristics. It also includes a new representation of noise levels for secondary phases that is based on the coda of previous arrivals.

### 2.2 Detection Module

The detection module calculates the signal and noise amplitudes for each wave, station, and epicenter. These amplitudes are used to determine the probability of detection at individual stations. The individual station probabilities are combined to determine the probability of detection for the network. The *NetSim* detection algorithm is essentially the same as that of *SNAP/D* and *SNAP/DX*. However, there are two main exceptions. First, the signal and noise amplitudes at individual stations are calculated as a function of frequency. Second, the noise for secondary phases depends on the amplitude spectrum of previous arrivals and the coda decay rate. Therefore, the noise for secondary phases depends on event magnitude and epicentral distance.

The *NetSim* detection module has two options. It can calculate the detection threshold of the network at a fixed confidence level (these thresholds are determined by varying the event size until the detection probability of the network equals the desired confidence level), or it can calculate the probability that the network will detect an event of fixed size. In either case, the calculations are performed for each epicenter in a grid specified by the user. The results are displayed on a map, either as contours of event size (for fixed confidence level), or as contours of detection probability (for fixed event size).

The first step in the detection module is to calculate the probability of detection at individual stations. Assuming that both signal and noise are log normally distributed, the probability that wave  $k$  will be detected at station  $i$  from an event at epicenter  $j$  is:

$$P_{ijk} = R_i \phi \left[ \frac{\log S_{ijk} - \log N_{ijk} - \log \text{SNR}_{ik}}{(\sigma_{S_{ijk}}^2 + \sigma_{N_{ijk}}^2)^{1/2}} \right] \quad (2.2.1)$$

where,

$$\phi(x) = \frac{1}{\sqrt{2\pi}} \int_{-\infty}^x e^{-y^2/2} dy \quad (2.2.2)$$

and,

- $R_i$  = reliability of station  $i$  (the fraction of time that station  $i$  is operational).
- $S_{ijk}$  = signal amplitude for wave  $k$  at station  $i$  from epicenter  $j$ .
- $N_{ijk}$  = noise amplitude for wave  $k$  at station  $i$  from epicenter  $j$ .
- $\text{SNR}_{ik}$  = signal-to-noise ratio necessary for detection of wave  $k$  at station  $i$ .
- $\sigma_{S_{ijk}}$  = standard deviation of log signal amplitude for wave  $k$  at station  $i$  from epicenter  $j$ .
- $\sigma_{N_{ijk}}$  = standard deviation of log noise amplitude for wave  $k$  at station  $i$  from epicenter  $j$ .

The signal and noise amplitudes at individual stations are calculated at frequencies selected by the user. The individual station probabilities in (2.2.1) are evaluated at the frequency that maximizes the signal-to-noise ratio, and this frequency is generally a function of distance. The individual station probabilities are combined to determine the probability of detection for the network. This calculation is the same as the *SNAP/D* implementation which has already been described in detail by *Ciervo et al.* [1985]. The calculation of the signal and noise amplitudes and standard deviations are described in the following two sections.

### 2.2.1 Signal

The signal amplitudes at individual stations  $S_{ijk}$  are calculated using one of two equations depending on whether the  $j$ th epicenter is at a regional or teleseismic distance from the  $i$ th station (the crossover distance is selected by the user). For regional distances:

$$\log S_{ijk}(f) = \log C_{ijk} + s_{jk}(f) + B_k(\Delta_{ij}, f) + SR_{ik}(f) + \text{stacor}_{ik} \quad (2.2.3)$$

where  $C_{ijk}$  is a constant that depends on the physical properties of the source and

receiver media,  $s_{jk}(f)$  is the log source spectrum for the  $k$ th wave,  $B_k(\Delta_{ij}, f)$  is the attenuation of the  $k$ th wave as a function of epicentral distance  $\Delta_{ij}$  and frequency  $f$ , and  $SR_{ik}(f)$  is a combination of the local site response and array gain as a function of frequency for the  $k$ th wave observed at the  $i$ th station. Each of these terms are described in more detail below. The last term in (2.2.3),  $stacor_{ik}$ , is an amplitude station correction for the  $k$ th wave at the  $i$ th station.

The constant  $C_{ijk}$  is expressed as [e.g., *Aki and Richards*, 1980]:

$$C_{ijk} = \frac{10^9}{4\pi (\rho_j \rho_i v_{jk}^5 v_{ik})^{1/2}} \quad (2.2.4)$$

where  $\rho_j$  and  $\rho_i$  are the densities of the source and receiver media, respectively. Similarly,  $v_{jk}$  and  $v_{ik}$  are the seismic velocities of the  $k$ th wave at source and receiver, respectively. The velocity and density at the  $j$ th epicenter are determined from a source medium geographical grid, and the velocity and density of the  $i$ th station are determined from a list of station parameters. The factor of  $10^9$  in (2.2.4) converts amplitudes from meters to nanometers.

The source spectrum is represented as a product of a wave-independent moment spectrum  $M_0(f)$  and a wave-dependent excitation factor,  $\kappa_k$ . Specifically, the log source spectrum is expressed as:

$$s_{jk}(f) = \log \kappa_k + \log M_0(f) \quad (2.2.5)$$

Both  $\kappa_k$  and  $M_0$  depend on the source medium (for example, different source spectra are used for explosions in salt, granite, or tuff). The factor  $\kappa_k$  represents the relative source excitation of different wave types (e.g., typical values for explosions are 1.0 for  $P$  phases and 0.3 for  $S$  phases).

The  $B_k(\Delta_{ij}, f)$  are frequency-dependent amplitude versus distance curves. Separate curves are tabulated for each wave and for each propagation medium (e.g., stable or tectonic). A propagation grid identifies the geographical locations of these different propagation media. The effective attenuation for each wave used in (2.2.3) is a linear combination of the separate  $B_k(\Delta_{ij}, f)$  for each propagation medium between the  $j$ th epicenter and the  $i$ th station. The path weights applied to the separate attenuation curves are calculated from the relative portion of the great circle path in each propagation medium [*Ciervo et al.*, 1985].

The local site response spectrum  $SR_{ik}(f)$  includes effects such as free surface amplification, instrument response, and array gain. Since the signal-to-noise ratio is used to determine detection probabilities at individual stations, the actual instrument response spectrum is not needed. Instead, the instrument response portion of  $SR_{ik}(f)$  is set to zero for frequencies included in the instrument passband, and it is set to a large negative number for frequencies outside the instrument passband. This is useful for

representing the capability of networks that include both broad band and narrow band stations. It is also important to represent the capability of networks that include both single stations and regional arrays. For single stations, the array gain portion of  $SR_{ik}(f)$  is set to zero for all frequencies. However, since beamforming can be very effective in suppressing uncorrelated noise [e.g., *Kvearna*, 1989], the array gain portion of  $SR_{ik}(f)$  will generally be greater than zero for array stations. For example, if beamforming results in  $\sqrt{N}$  noise suppression, and if the signal is perfectly coherent across the array, then  $SR_{ik}(f) = 1/2 \log N$ . Since signal coherence (and the number of array elements used in beamforming) generally decrease with increasing frequency,  $SR_{ik}(f)$  is expected to decrease with frequency for array stations.

The signal amplitude at teleseismic distances has a slightly different representation than the signal amplitude at regional distances (2.2.3). For teleseismic distances the signal amplitude is expressed as:

$$\log S_{ijk}(f) = \log C_{ijk} + s_{jk}(f) + B_k^{\text{REF}}(\Delta_{ij}, f) + SR_{ik}(f) + stacor_{ik} + Scorer_{jk} + Rcor_{ik} \quad (2.2.6)$$

There are two main differences between this representation and the corresponding relation for regional distances. First, the path-weighted amplitude versus distance curve in (2.2.3) is replaced with a reference amplitude versus distance curve  $B_k^{\text{REF}}(\Delta_{ij}, f)$  that is used for all source-receiver paths. This assumes that strong lateral variations in the earth are confined to shallow structure, so that teleseismic waves (which propagate at greater depth) travel primarily in a laterally homogeneous medium. The second difference is that the teleseismic representation includes source and receiver amplitude correction factors ( $Scorer_{jk}$  and  $Rcor_{ik}$ ) that depend on the propagation medium of the  $j$ th epicenter and  $i$ th station. These factors are used to model the effects of near-source and near-receiver geology that can, for example, introduce a magnitude bias between two receiver or source sites.

The variance of the log signal amplitude for each wave is the sum of the variance of the amplitude versus distance relation  $\sigma_{B_k(\Delta_{ij})}^2$  and the station-specific log amplitude variance  $\sigma_{ik}^2$ . That is,

$$\sigma_{S_{ijk}}^2 = \sigma_{B_k(\Delta_{ij})}^2 + \sigma_{ik}^2 \quad (2.2.7)$$

For regional distances, the variance of the amplitude-distance relation is a linear combination of the variances for the individual propagation media. The weights are determined from the portion of the great circle path between source and receiver in each propagation medium.

### 2.2.2 Noise

The noise spectrum for each wave and station is expressed as a sum of the ambient noise spectrum and (for secondary phases) a signal-generated noise spectrum which includes the coda of the previous arrival. This signal-generated noise spectrum depends both on event size and epicentral distance. The noise power spectral density for each wave, station, and epicenter is expressed as:

$$PSD_{ijk}(f) = PSDa_i(f) + PSDs_{ijk}(f) \quad (2.2.8)$$

where  $PSDa_i(f)$  is the power spectral density of the ambient noise at the  $i$ th station, and  $PSDs_{ijk}(f)$  is the power spectral density of the signal-generated noise for the  $k$ th wave at the  $i$ th station from the  $j$ th epicenter.

The frequency content of the signal-generated noise for secondary phases is expected to be much different from the frequency content of the ambient noise, and similar to the frequency content of the previous arrival. Also, the amplitude of the noise for secondary phases depends on the amplitude of the previous arrival and on the coda decay rate. The simplest assumption consistent with these dependencies is that the signal-generated noise spectrum for secondary phases is equal to the signal spectrum of the previous arrival multiplied by a scaling factor that depends on distance (or, equivalently, on the time separation between the secondary phase and the previous arrival). This is the assumption used by *NetSim* to determine noise levels for secondary phases. The power spectral density of the signal-generated noise is calculated from the amplitude spectrum of the previous arrival  $S_{ij(k-1)}$  using:

$$PSDs_{ijk}(f) = \frac{[\gamma_k(\Delta_{ij}) S_{ij(k-1)}]^2}{T_{(k-1)}} \quad (2.2.9)$$

where  $\gamma_k(\Delta_{ij})$  is the coda decay rate, and  $T_{(k-1)}$  is the time window length used to calculate the signal spectrum of the previous arrival. This parameterization assumes that the coda decay rate does not depend on frequency. A more complicated model that includes frequency dependence in  $\gamma_k$  could also be adopted if it is found that this is important for simulating the capability to detect regional secondary phases.

It is straight forward to calculate the noise amplitude spectrum from the noise power spectral density. The relationship is:

$$N_{ijk}(f) = [T_k PSD_{ijk}(f)]^{1/2} \quad (2.2.10)$$

where  $PSD_{ijk}(f)$  is calculated using (2.2.8) and (2.2.9), and  $T_k$  is the time window length used to calculate the signal spectrum for the  $k$ th wave. The noise spectrum in (2.2.10) is used in (2.2.1) to calculate the probability of detection at individual stations.

The standard deviation of the log noise amplitude is a function of the standard deviation of the log ambient noise at each station, and (for secondary phases) the standard

deviation of the log signal amplitude of the previous wave. Assuming that signal and noise are log normally distributed, the standard deviation of the log noise for the  $k$ th wave at the  $i$ th station from an event at the  $j$ th epicenter is:

$$\sigma_{N_{ik}} = \frac{\left[ PSDa_i(f)^2 \sigma_{N_{ai}}^2 + PSDs_{ijk}(f)^2 \sigma_{S_{ij(k-1)}}^2 \right]^{1/2}}{PSDa_i(f) + PSDs_{ijk}(f)} \quad (2.2.11)$$

where  $\sigma_{N_{ai}}$  is the standard deviation of the log ambient noise amplitude at the  $i$ th station, and  $\sigma_{S_{ij(k-1)}}$  is the standard deviation of the log signal amplitude of the previous wave. Note that as the signal-generated noise approaches zero, the standard deviation of the log noise for the  $k$ th wave approaches the standard deviation of the log ambient noise.

### 2.3 Location Module

*NetSim* estimates location capability by computing the dimensions of the hypocentral confidence ellipsoid for each epicenter in the grid. The location uncertainty can be calculated at fixed event size, or at the detection threshold of the network. In the latter case, the detection module is used to calculate the detection threshold for each epicenter before activating the location module. This section gives a brief description of the calculations performed by the *NetSim* location module. More details are given by *Bratt et al.* [1987a] and *Bratt and Bache* [1988]. Section 2.3.1 describes the probability-weighted location uncertainties (the method used by *SNAP/D*) and Section 2.3.2 describes the Monte Carlo approach for estimating location uncertainties.

The location confidence bounds depend on the distribution of the detecting stations, the presumed earth structure, and *a priori* estimates of the data variance. Effects of network geometry and earth structure are reflected in the matrix of partial derivatives of the data with respect to the hypocentral coordinates and origin time [*Bratt et al.*, 1987a]. Traditionally, data have been phase arrival times. However, azimuth data from arrays or three-component stations can also provide significant constraint on location solutions. In fact, under conditions where few data are available they permit event locations not possible using arrival-time data alone.

The *NetSim* location algorithm computes location uncertainties using both arrival time and azimuth partial derivatives for any seismic phase [*Bratt et al.*, 1987a]. If the data variances are assumed to be known *a priori* (an assumption required for network simulation), then the points  $x_e$  on the  $p$  percent confidence ellipsoid for the solution  $x$  are obtained from

$$(x_e - x)^T V_x^{-1} (x_e - x) = \chi_p^2 [M] \quad (2.3.1)$$

where  $\chi_p^2 [M]$  is the  $p$  percent chi-squared statistic with  $M$  degrees of freedom ( $M$  is the number of hypocentral parameters) and  $V_x$  is an estimate for the parameter covariance matrix [e.g., *Jordan and Sverdrup*, 1981; *Bratt and Bache*, 1988]. The arrival time

and azimuth variances for each wave are a sum of the station-specific variances and the variances that depend on the propagation media between the source and receiver. The path weights are determined from the relative fraction of the great circle path in each medium.

In the simulations the individual stations have some probability ( $\leq 100\%$ ) of detecting an event, but in practice a phase is either detected and used in the location solution or it is not detected and cannot be used to constrain location. *NetSim* offers two ways in which the probability of detecting a given phase can be used to estimate location uncertainties. One of these ways is by weighting the standard deviation of each datum by the square root of the probability of detection [Ciervo *et al.*, 1985]. Another way is to compute a large number of confidence ellipses at each epicenter, using subsets of all detections selected in a random or *Monte Carlo* fashion based on the probability of detection [Bratt *et al.*, 1987a]. These two methods are described in more detail in the following subsections.

### 2.3.1 Probability Weighting

In the probability-weighted approach, the effect of undetected phases is approximated by assuming that every phase is detected and produces data whose standard error is increased by a factor that depends on the probability of detection [Ciervo *et al.*, 1985]. The standard deviation of each datum  $\sigma$  is divided by the square root of the probability  $P_{ijk}$  that the station in question will detect that phase. The effective standard deviations ( $\sigma/\sqrt{P_{ijk}}$ ) are increased for phases with low probability of detection, and therefore these phases do not contribute much to constraining the event hypocenter.

The probability-weighted approach for computing average confidence bounds is most accurate when the parameters of the error ellipse are not very sensitive to the exclusion of an individual datum [Ciervo *et al.*, 1985]. However, when few data are available to locate an event (e.g., for most events near the detection threshold), each datum is very important. Thus, the accuracy of the probability-weighted location uncertainties degrades with decreasing event size. Bratt *et al.* [1987a] show that the probability-weighted approach increasingly underestimates the Monte Carlo uncertainties as the event size decreases, which suggests that this method does not adequately degrade the contribution of data with low detection probabilities.

### 2.3.2 Monte Carlo

The Monte Carlo approach does not assume that every phase is detected. Instead, a large number of confidence ellipses are calculated at each epicenter, and each realization includes data from a subset of all phases. The subset is determined by comparing the probability of detection at each station to a uniformly distributed random number between 0 and 1. If the probability of detection is greater than the random number, then the phase is included in the location confidence calculation. Otherwise, the phase is not detected and cannot be used to constrain location. From these realizations,

statistics such as the median and 90th percentile confidence bounds can be determined. This approach mimics the process by which average confidence ellipses would be obtained from many located events in a region, but it is more computationally intensive than the probability-weighted approach.

### 3. NETSIM INPUT/OUTPUT

This section gives a brief description of the *NetSim* input and output data, and the graphics capabilities. Appendix A lists the contents of each input and output data file and gives a more detailed description of each of the parameters.

Figure 3.1 is a schematic top-level data flow diagram for *NetSim*. The input data are organized into five categories:

- (1) Control Data
- (2) Source Data
- (3) Propagation Data
- (4) Site/Station Data
- (5) Noise Data

The data in each of these categories are described in Section 3.1. In general, each category includes several input files (indicated by the smallest boxes in Figure 3.1). There are a total of 13 different types of input files. Some of these files are indices (or pointers) and others are one-dimensional or two-dimensional data tables. Section 4 of this report gives examples of the input files for a few sample runs.

The output of the *NetSim* detection module is either detection thresholds for a fixed confidence level, or detection probability for a fixed event size. The location module outputs the parameters of the hypocentral confidence ellipsoid for a fixed confidence level. The *NetSim* output data are described in Section 3.2. A graphics package called *SnapCon* is used to contour the *NetSim* output on regional or world maps [Bratt *et al.*, 1987b]. The *SnapCon* graphics package is described in Section 3.3.

#### 3.1 Input Data

##### (1) Control Data

The control data determine what type of calculations are to be performed. There is only one input data file in this category (the control file, Figure 3.1). *NetSim* prompts for the name of the control file at the start of each run. The user is given an opportunity to view and/or modify the contents of this file, write any changes to disk, and to proceed by reading the rest of the input data files.

The control data include the *NetSim* run type which is either *detection*, *location*, or *detloc* (detection and location). If the run type is set to *detection*, then the location module is not activated. However, if the run type is set to *location*, the detection module must calculate the individual station probabilities since these are needed to estimate location uncertainty. If the run type is set to *detloc* then both modules are activated, and the location uncertainties for each epicenter are calculated at the

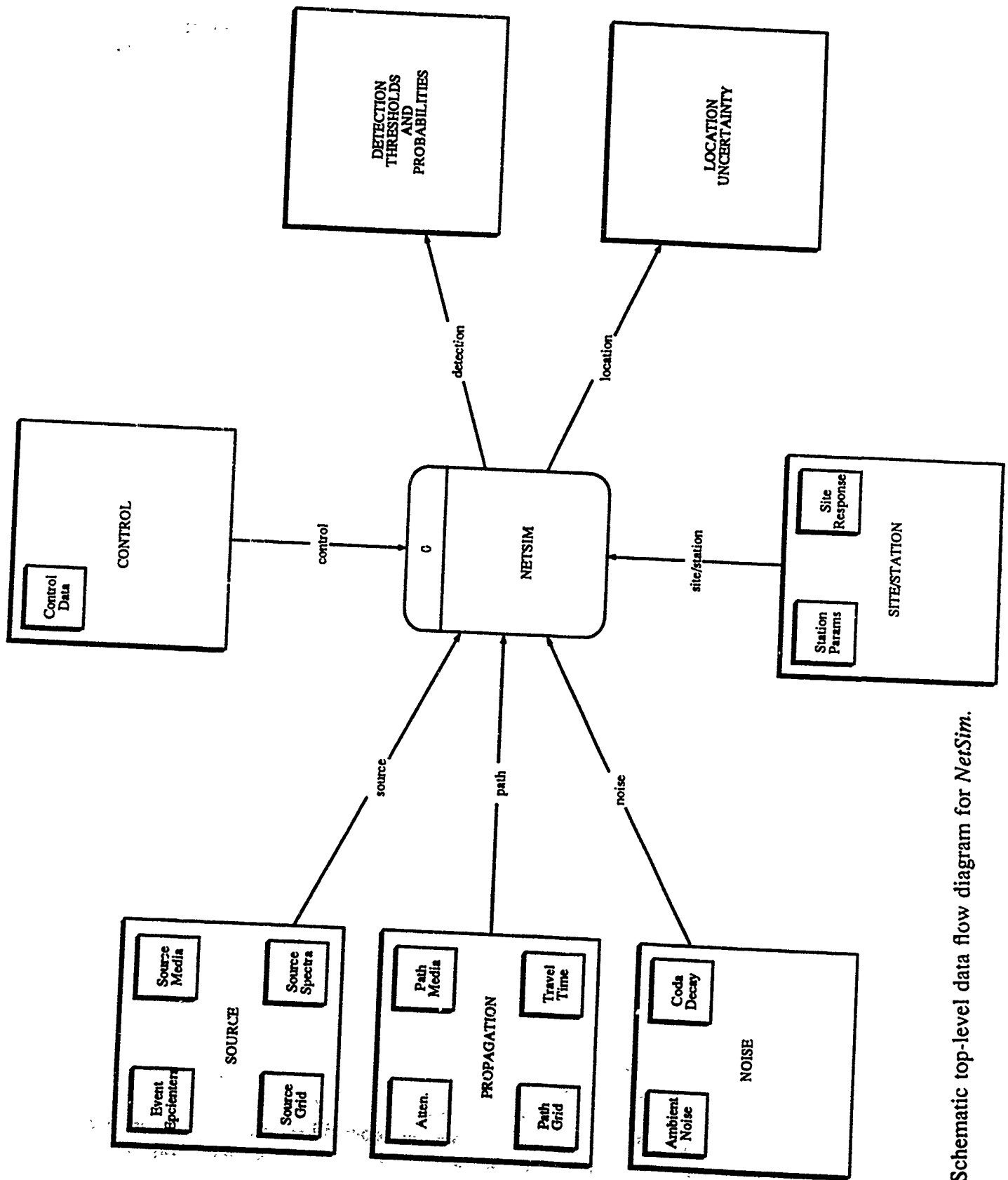


Figure 3.1. Schematic top-level data flow diagram for NetSim.

detection threshold for the network. The run subtype is also included in the control input. This is either *threshold* (to calculate the detection threshold at fixed confidence level), or *probability* (to calculate the probability of detection for fixed event size). Note that event size can be represented in terms of explosion yield, seismic moment,  $m_b$ ,  $M_s$ , or  $MLg$ . The conversions between these measures are included in the input data for each source medium. Other control data include the detection criteria (e.g., the wave types and number of stations required for detection), probability of detection for the network (for a threshold run), event size (for a probability or location run), location confidence level, number of Monte Carlo realizations (=1 for probability-weighting), frequencies to include in the calculation, and the names of the input data files.

## (2) Source Data

The source data are used to calculate the excitation of each wave as a function of frequency and source medium,  $s_{jk}(f)$ . There are four input file types in this category: epicenter grid file, source medium file, source medium grid file, and the source spectra files.

The epicenter grid file specifies the event epicenters at which to calculate the detection thresholds, probability of detection, or location uncertainties. The source medium file specifies source scaling and excitation factors for each source medium. This includes the medium name (e.g., granite, tuff, salt), the file name for the source spectrum, the density and velocity of the source medium, the scaling relations between log moment and other measures of event size (yield,  $m_b$ ,  $M_s$ , and  $MLg$ ), and the excitation factors for each wave,  $\kappa_k$ . The source grid file identifies the geographic locations of each source medium. The source spectra for each source medium are stored in two-dimensional data files that tabulate  $M_0(f)$  as a function of scalar seismic moment and frequency.

## (3) Propagation Data

The propagation data are used to determine the frequency-dependent attenuation  $B_k(\Delta_{ij})$  and travel times (and their standard deviations) for each wave as a function of path medium. There are four input file types in this category: path medium file, path medium grid file, attenuation files, and travel time files.

The path medium file specifies attenuation and travel time parameters for each path medium. This includes the medium name (e.g., tectonic or stable), file names for attenuation and travel times for each wave, the standard deviation of the attenuation curves for each wave, the travel time and azimuth standard deviations, and the source and receiver amplitude correction factors for teleseismic distances. The path grid file identifies the geographic locations of each path medium. The attenuation  $B_k(\Delta_{ij})$  for each wave and path medium is tabulated in two-dimensional data files as a function of

distance and frequency. The travel times are tabulated as a function of depth and distance.

#### (4) Site/Station Data

The site/station data include the local site response for each station  $SR_{ik}$  (which includes the free surface amplification, instrument response, and the frequency-dependent beam gain for array stations), and individual station parameters. There are two input files in this category: station file and site response file.

The station file includes the names and geographical coordinates of each station, file names for ambient noise spectra, the standard deviation of log noise, station reliability, amplitude station corrections, signal-to-noise ratio required for detection of each wave, station-specific standard deviations (travel time, azimuth, and log amplitude), file names for coda decay rates, and file names for the site response for each wave and station. The site response is tabulated in a one-dimensional data file as a function of frequency.

#### (5) Noise Data

The noise data define the ambient station noise spectra and the coda decay rates used to calculate noise spectra for secondary phases. There are two input files in this category: the ambient noise file and the noise factor file for secondary phases. Both of these files are indexed in the station file.

There is a separate ambient noise file for each station. These files tabulate ambient noise power spectral density as a function of frequency. The noise factor file for secondary phases tabulates the coda decay rate of the previous arrival as a function of distance,  $\gamma_k(\Delta_{ij})$ .

### 3.2 Output Data

*NetSim* writes two types of output files; a graphics file used by *SnapCon* to display the results as contours on a map (Section 3.3), and a list file that contains detailed information about the detection and location parameters for each epicenter and for each station. The graphics file is called *prefix.gra* and the list file is called *prefix.lst*, where *prefix* is specified in the control input.

The graphics file includes a table that lists event size, probability of detection for the network, and location uncertainties for each epicenter in the grid. For threshold runs, the event size is equal to the detection threshold for the network. Otherwise, it is equal to the fixed value specified in the control input (e.g., for probability or location runs). The location uncertainties are reported as the length of the semi-major and semi-minor axes of the epicenter location error ellipse, the strike of the semi-major

axis, and the depth uncertainty. For *Monte Carlo* simulations, the fraction of simulations with enough data to locate the event is also reported in the graphics file.

The list file includes all of the information contained in the graphics file and information about the detection and location capabilities of individual stations in the network. The list file includes the following information for each station, wave and epicenter: detection probability  $P_{ijk}$ , epicentral distance and event azimuth, frequency of the maximum signal-to-noise ratio, standard deviation of log amplitude, azimuth and arrival time standard deviation, and depth and epicenter importances [Ciervo *et al.*, 1985].

### 3.3 Graphics

*SnapCon* is a graphics package developed by Bratt *et al.* [1987b] to plot *SNAP/D* results as contours on regional and world maps. Normally, *SnapCon* is used to contour detection thresholds or location uncertainties. However, it can also be used to contour the difference or percentage change between two simulation runs. Using these options, it is possible to estimate the change in detection capability due to changes in input parameters such as network geometry, detection criteria, or attenuation curves. *SnapCon* uses the NCAR (National Center for Atmospheric Research) graphics library with enhancements by MINEsoft, Ltd. *SnapCon* can be used to generate one or more plots during a single run, and these plots are stored in a *metacode* graphics output file. These *metacodes* can be plotted on selected output devices (e.g., SunView or PostScript) using metacode translation programs.

The *NetSim* output graphics file has a slightly different format than the *SNAP/D* output graphics file, so we made minor modifications to *SnapCon* so that we could use it to contour *NetSim* results. This new version of *SnapCon* has the same functionality as the version described in the *SnapCon* user's and programmer's guide written by Bratt *et al.* [1987b]. Examples of *SnapCon* graphics are given in Section 4 of this report.

Bratt *et al.* [1987c] describe a graphics package (also based on the NCAR graphics library) to plot *SNAP/D* results stored in the list file. This package, called *PRIMP*, plots the probability of detecting each wave at individual stations for a given epicenter ( $P_{ijk}$ ), and location importances which measure the relative contribution of a particular datum to event location. These plots are useful for determining detection and location capabilities of individual stations in the network. However, we have not yet modified the *PRIMP* graphics package to read the list file generated by *NetSim*.

(THIS PAGE INTENTIONALLY LEFT BLANK)

## 4. SAMPLE RUNS

This section presents sample *NetSim* and *SnapCon* runs for frequency-independent and frequency-dependent input. *The simulations presented in this section are only illustrative examples of the NetSim computer program. These simulations are not intended to represent accurate estimates of the detection and location capability of seismic networks in the Soviet Union.* Instead, the examples in this section illustrate the main functionality of *NetSim*, the importance of frequency dependence for simulating capability at regional distances, and the inability of the probability-weighted (*SNAP/D*) approach to properly account for the effect of undetected phases on location uncertainties for events near the detection threshold of the network.

Section 4.1 presents sample *NetSim* runs at fixed frequency. The results for two separate calculations (1 Hz and 10 Hz) are compared. Included in that section are listings of the input and output data files, and a complete transcription of an interactive *NetSim* session. Section 4.2 presents simulations for frequency-dependent input, and compares them to the simulations for fixed frequency presented in Section 4.1. Section 4.3 compares location uncertainties computed using the probability-weighted approach to those computed using the Monte Carlo approach.

### 4.1 Frequency-Independent Input

This section describes sample *NetSim* calculations for fixed frequency. These calculations have been compared to *SNAP/D* calculations to verify that these programs give the same output when they are given identical (frequency-independent) input. The main purpose of this section is to give examples of the input and output files for *NetSim*, and to illustrate the *NetSim* data handling and user-interface modules.

#### INPUT DATA

The input parameters described here are frequency-dependent. However, the simulations presented in this section are calculated for a single frequency, so they are the same as simulations for frequency-independent input (e.g., like *SNAP/D* simulations). The advantage of using frequency-dependent input data files is that they can be used without modification to simulate broad band detection capability (as demonstrated in the next section) or detection capability at any fixed frequency. The sample input data files in each of the five categories (control, source, propagation, site/station, and noise) are described below. None of the sample runs include secondary phases, so the only wave-dependent parameters included in the sample input files are for *P* phases. These sample data files are based on our experience with the NORESS array in Norway [Serenio *et al.*, 1988]. However, we have extrapolated our NORESS results to much larger distances and somewhat higher frequencies. Therefore, the simulations have large uncertainty (particularly for events near the periphery of the network) and should not be interpreted as accurate estimates of detection capability in the Soviet Union.

**Control Data.** Table 4.1 lists the contents of the sample control file. This file specifies that the 90%  $ML_g$  thresholds for detecting 3  $P$  phases at 1.0 Hz will be calculated. Magnitude search bounds are 1.0 and 8.0. The names of other input files are listed at the bottom of the control file.

**Source Data.** Table 4.2 lists the contents of the four source data files (epicenter grid, source media, source grid, and source spectra). These files specify:

- A  $15^\circ \times 15^\circ$  epicenter grid for Eurasia
- Homogeneous granite source medium grid
- Source medium properties (granite)
  - Density =  $2500 \text{ kg/m}^3$
  - Compressional wave velocity =  $5000 \text{ m/s}$
- Source scaling relations (granite)
  - $\log M_0 = 1.08 ML_g + 10.6$
  - $P$ -wave excitation factor,  $\kappa = 1.0$
  - Source spectra as a function of  $\log M_0$  (Figure 4.1)

**Propagation Data.** Table 4.3 lists the contents of the four propagation data files (path media, path grid,  $P$ -wave attenuation, and  $P$ -wave travel times). These files specify:

- Homogeneous propagation characteristics (stable)
- Window length for  $P$  wave spectra =  $5.0 \text{ s}$
- Standard deviations for  $P$  phases
  - Log amplitude standard deviation =  $0.3$
  - Arrival time standard deviation =  $1.5 \text{ s}$
  - Azimuth standard deviation =  $8.0^\circ$
- $P$ -wave attenuation versus frequency (Figure 4.2)
- $P$ -wave travel times

**Site/Station Data.** Table 4.4 lists the contents of the two site/station data files (station, site response). These specify:

- A network of 20 internal and 13 external arrays (Figure 4.3)
- The same ambient noise spectra and standard deviation for all stations
- A  $P$ -wave SNR for detection =  $4.0$  for all stations
- Receiver medium properties for all stations
  - Density =  $2500 \text{ kg/m}^3$
  - Compressional wave velocity =  $5000 \text{ m/s}$

CONTROL DATA

CONTROL FILE: ./firun1.cnt

Frequency-Independent Detection Thresholds  
FIRun1  
./results  
./  
detection  
threshold  
(P/3)  
P  
mlg  
3.000 1.000 8.000 0.900 0.000 20.000  
0.900 100 0.500 0.900  
fixed 0.000  
1  
1.000  
euras.epi  
granite.smd  
granite.sgr  
stable.pmd  
stable.pgr  
a20x13.sta

Table 4.1. Sample control data.

SOURCE DATA

EPICENTER FILE: ./euras.epi

Eurasia Epicenters  
 7 13  
 0.000 0.000  
 15.000 15.000

SOURCE MEDIA FILE: ./granite.smd

Granite Source Media  
 ./srctab  
 1  
 granite  
 expl.sor  
 2500.000  
 0.000 0.000 0.000 0.000 0.000 0.000 1.080 10.600  
 1.000 0.000 0.000 0.000 0.000 0.000 0.000 0.000  
 0.000 0.000  
 5000.000 0.000 0.000 0.000 0.000 0.000 0.000 0.000  
 0.000 0.000

SOURCE GRID FILE: ./granite.sgr

Granite Source Media Grid (5x5 degree)  
 36 72  
 -90.000000 -180.000000  
 5.000000 5.000000  
 granite -90.000000 -180.000000  
 granite -90.000000 -175.000000  
 granite -90.000000 -170.000000  
 : :  
 : :  
 granite 85.000000 165.000000  
 granite 85.000000 170.000000  
 granite 85.000000 175.000000

SOURCE SPECTRA FILE: ./srctab/expl.sor

Explosion Source  
 20  
 1.000 2.000 3.000 4.000 5.000 6.000 7.000 8.000  
 9.000 10.000 11.000 12.000 13.000 14.000 15.000 16.000  
 17.000 18.000 19.000 20.000  
 6  
 11.000 12.000 13.000 14.000 15.000 20.000  
 Source amplitudes for frequency = 1.00000  
 11.000 12.000 13.000 14.001 15.003 17.912  
 Source amplitudes for frequency = 2.00000  
 11.000 12.000 13.001 14.002 15.002 17.310  
 : : : : : :  
 : : : : : :  
 Source amplitudes for frequency = 18.0000  
 11.002 12.003 12.910 13.401 13.737 15.401  
 Source amplitudes for frequency = 19.0000  
 11.002 12.002 12.890 13.356 13.690 15.354  
 Source amplitudes for frequency = 20.0000  
 11.002 12.002 12.867 13.312 13.645 15.310

Table 4.2. Sample source data.

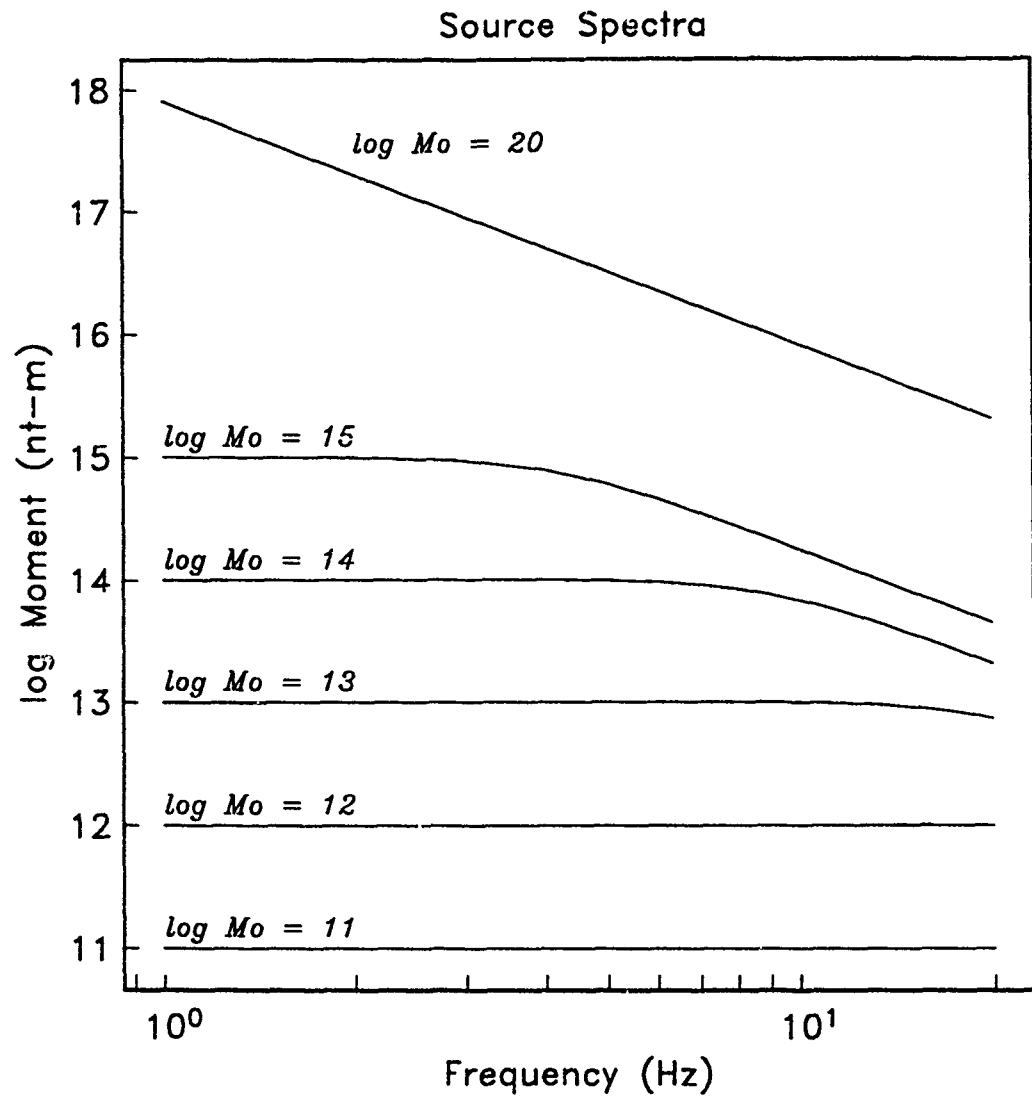


**Figure 4.1.** Input source spectra as a function of scalar seismic moment,  $M_0$ . Each curve is labeled by  $\log M_0$ . The corner frequency scales inversely with the cube root of the long-period level. The source scaling is from *Sereno et al.* [1988]. These spectra are stored in a two-dimensional data table called *expl.sor* (Table 4.2).



ATTENUATION FILE: ./pathtab/pstable.atn

stable - p

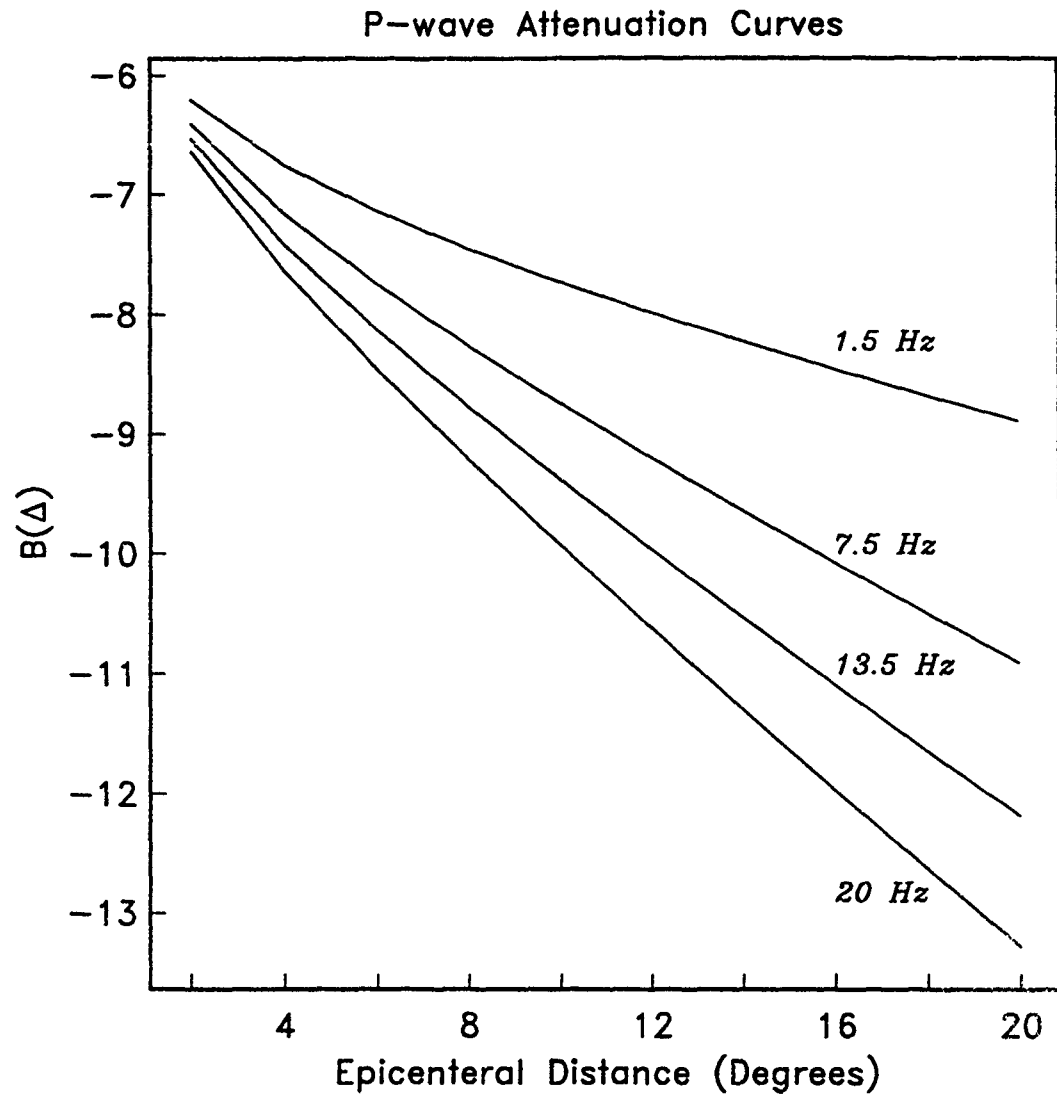
20	0.500	1.500	2.500	3.500	4.500	5.500	6.500	7.500
	8.500	9.500	10.500	11.500	12.500	13.500	14.500	15.500
	16.500	17.500	18.500	20.000				
50	0.000	2.000	4.000	6.000	8.000	10.000	12.000	14.000
	16.000	18.000	20.000	22.000	24.000	26.000	28.000	30.000
	32.000	34.000	36.000	38.000	40.000	42.000	44.000	46.000
	48.000	50.000	52.000	54.000	56.000	58.000	60.000	62.000
	64.000	66.000	68.000	70.000	72.000	74.000	76.000	78.000
	80.000	82.000	84.000	86.000	88.000	90.000	92.000	94.000
	96.000	98.000						
Attenuation for frequency	0.500000							
	0.000	-6.138	-6.617	-6.933	-7.182	-7.395	-7.585	-7.759
	-7.922	-8.076	-8.222	-8.363	-8.499	-8.631	-8.760	-8.886
	-9.010	-9.131	-9.251	-9.368	-9.484	-9.599	-9.712	-9.824
	-9.936	-10.046	-10.155	-10.263	-10.371	-10.478	-10.584	-10.690
	-10.795	-10.899	-11.003	-11.106	-11.209	-11.312	-11.414	-11.516
	-11.617	-11.718	-11.819	-11.919	-12.019	-12.119	-12.219	-12.318
	-12.417	-12.516						
	:	:	:	:	:	:	:	:
	:	:	:	:	:	:	:	:
Attenuation for frequency	20.0000							
	0.000	-6.644	-7.628	-8.450	-9.206	-9.925	-10.620	-11.300
	-11.969	-12.628	-13.281	-13.927	-14.569	-15.208	-15.842	-16.474
	-17.104	-17.731	-18.356	-18.979	-19.601	-20.222	-20.841	-21.459
	-22.076	-22.692	-23.307	-23.921	-24.535	-25.147	-25.760	-26.371
	-26.982	-27.592	-28.202	-28.811	-29.420	-30.028	-30.636	-31.244
	-31.851	-32.458	-33.065	-33.671	-34.277	-34.882	-35.488	-36.093
	-36.698	-37.302						

TRAVEL TIME TABLE: ./pathtab/pstable.tim

Travel-time vs distance and depth - Pn stable

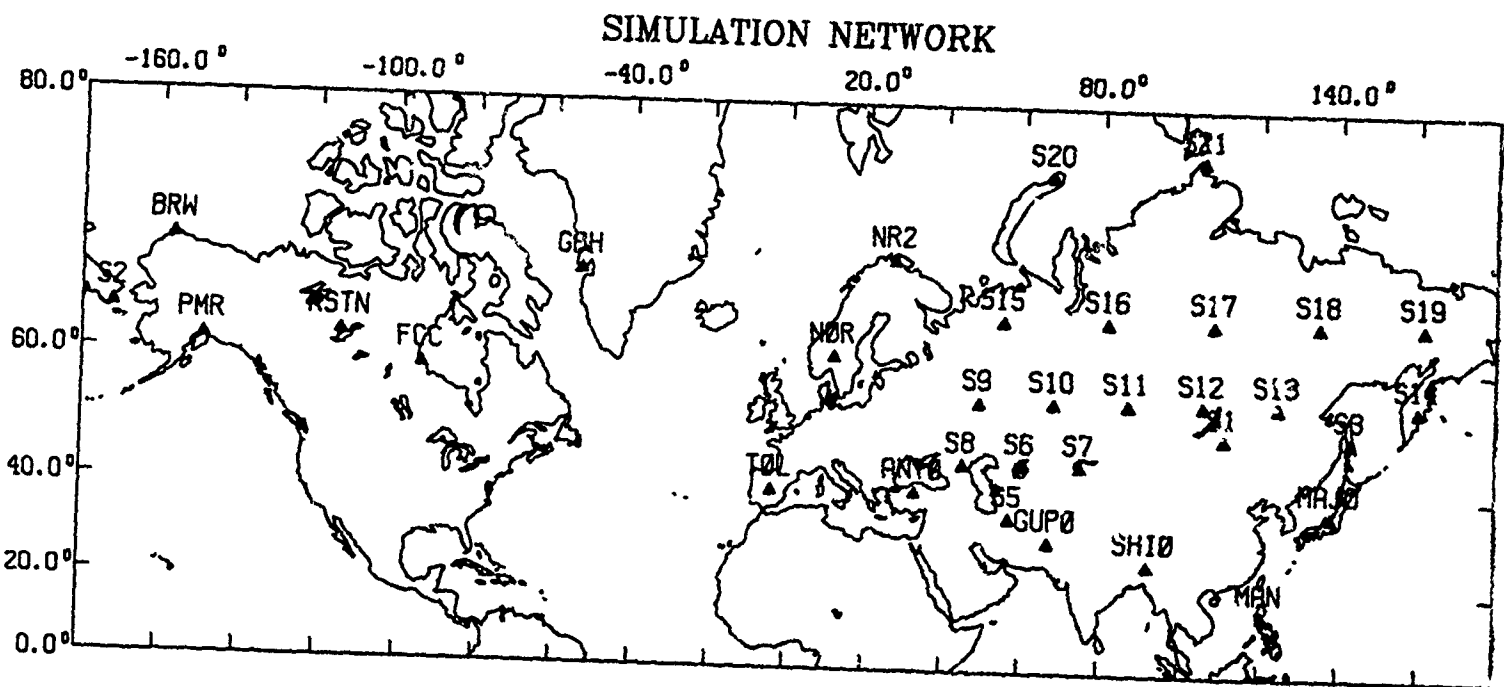
2	0.000	15.000						
181	0.000	1.000	2.000	3.000	4.000	5.000	6.000	7.000
	8.000	9.000	10.000	11.000	12.000	13.000	14.000	15.000
	:	:	:	:	:	:	:	:
	:	:	:	:	:	:	:	:
	168.000	169.000	170.000	171.000	172.000	173.000	174.000	175.000
	176.000	177.000	178.000	179.000	180.000			
Travel-time for source depth	0.							
	0.000	21.134	34.863	48.582	62.291	75.988	89.670	103.335
	116.978	130.597	144.189	157.752	171.289	184.775	198.199	211.480
	:	:	:	:	:	:	:	:
	:	:	:	:	:	:	:	:
	1206.987	1207.651	1208.261	1208.815	1209.314	1209.755	1210.140	1210.467
	1210.736	1210.946	1211.158	1211.253	1211.288			
Travel-time for source depth	15.0000							
	2.500	17.585	33.185	46.902	60.610	74.305	87.985	101.646
	115.286	128.902	142.490	156.048	169.579	183.058	196.466	209.722
	:	:	:	:	:	:	:	:
	:	:	:	:	:	:	:	:
	1204.488	1205.153	1205.762	1206.317	1206.815	1207.257	1207.642	1207.969
	1208.238	1208.448	1208.621	1208.713	1208.745			

Table 4.3. Sample propagation data (continued).



**Figure 4.2.** Input *P*-wave attenuation curves as a function of frequency. These curves are based on attenuation along paths to the NORESS array [Serenio *et al.*, 1988]. These  $B(\Delta, f)$  are stored in a two-dimensional data table called *pstable.atn* (Table 4.3).





**Figure 4.3.** Location of seismic stations comprising the hypothetical network used in our detection and location capability simulations. The station coordinates are stored in the station file, *a20x13.sta* (Table 4.4).

- Site response spectrum for all stations (Figure 4.4)

**Noise Data.** Table 4.5 lists the contents of one of the two noise data files (ambient noise). The other noise input file (noise factor for secondary phases) is not needed for this sample calculation since the detection criteria only include *P* waves. The ambient noise file is the power spectral density for all stations in the network (Figure 4.5).

#### NETSIM TRANSCRIPTION

A complete transcription of an interactive *NetSim* session that uses the input data files described above starts on page 31 of this report. Comments are separated from the transcription by a vertical line on each page. This transcription is included as examples of the *NetSim* data handling and user-interface modules.

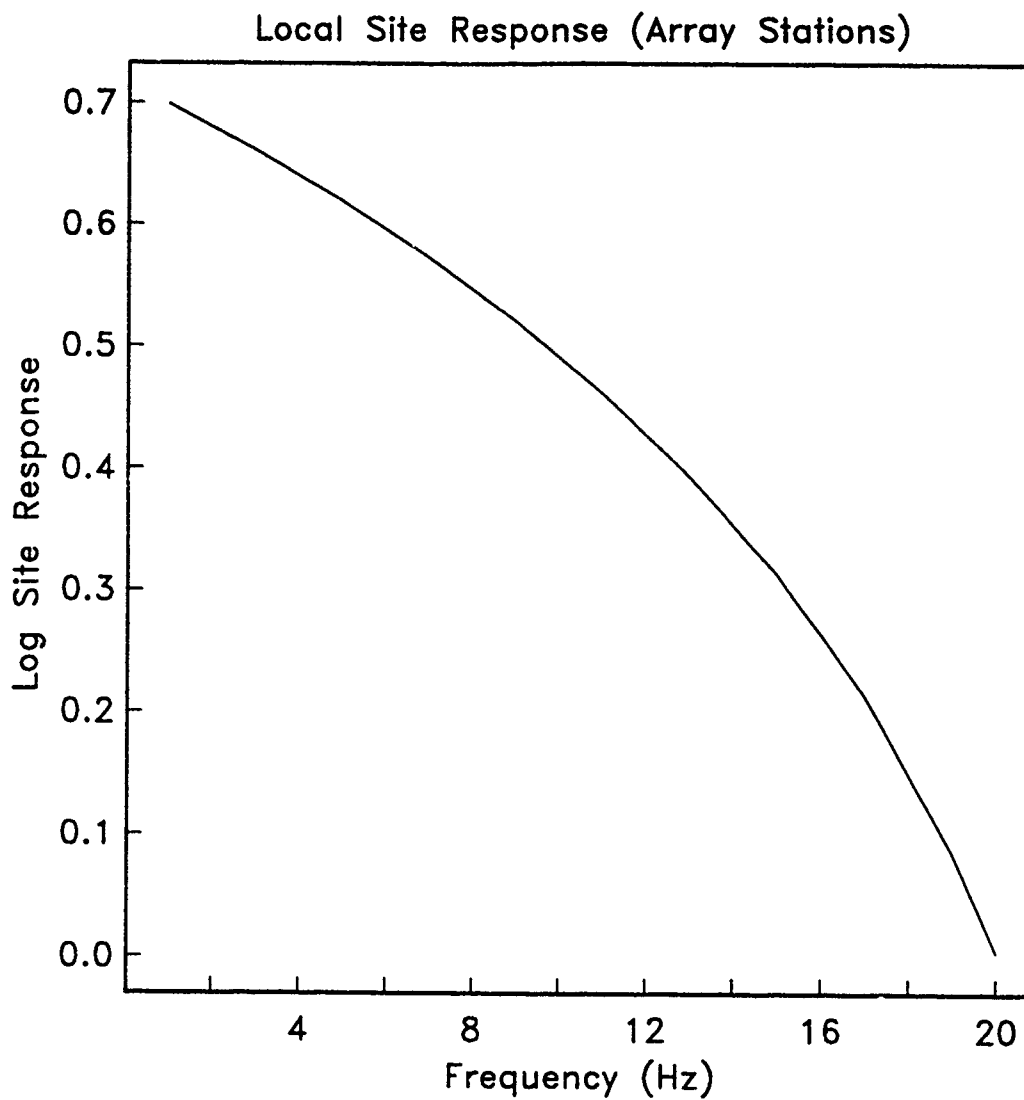


**Figure 4.4.** Input local site response for array stations. Only the array gain portion of the site response is included. We assume a linear decrease in beam gain from  $\sqrt{N}$  at 1 Hz to 1.0 at 20 Hz [Serenio *et al.*, 1988]. The site response as a function of frequency is stored in a one-dimensional data table called *array.srs* (Table 4.4).

NOISE DATA

AMBIENT NOISE FILE: ./station/ambient.no1

Ambient Noise, Noress	
253	
0.234	5.530
0.312	4.410
0.391	3.620
:	:
:	:
19.766	-5.550
19.844	-5.520
19.922	-5.460

Table 4.5. Sample noise data.

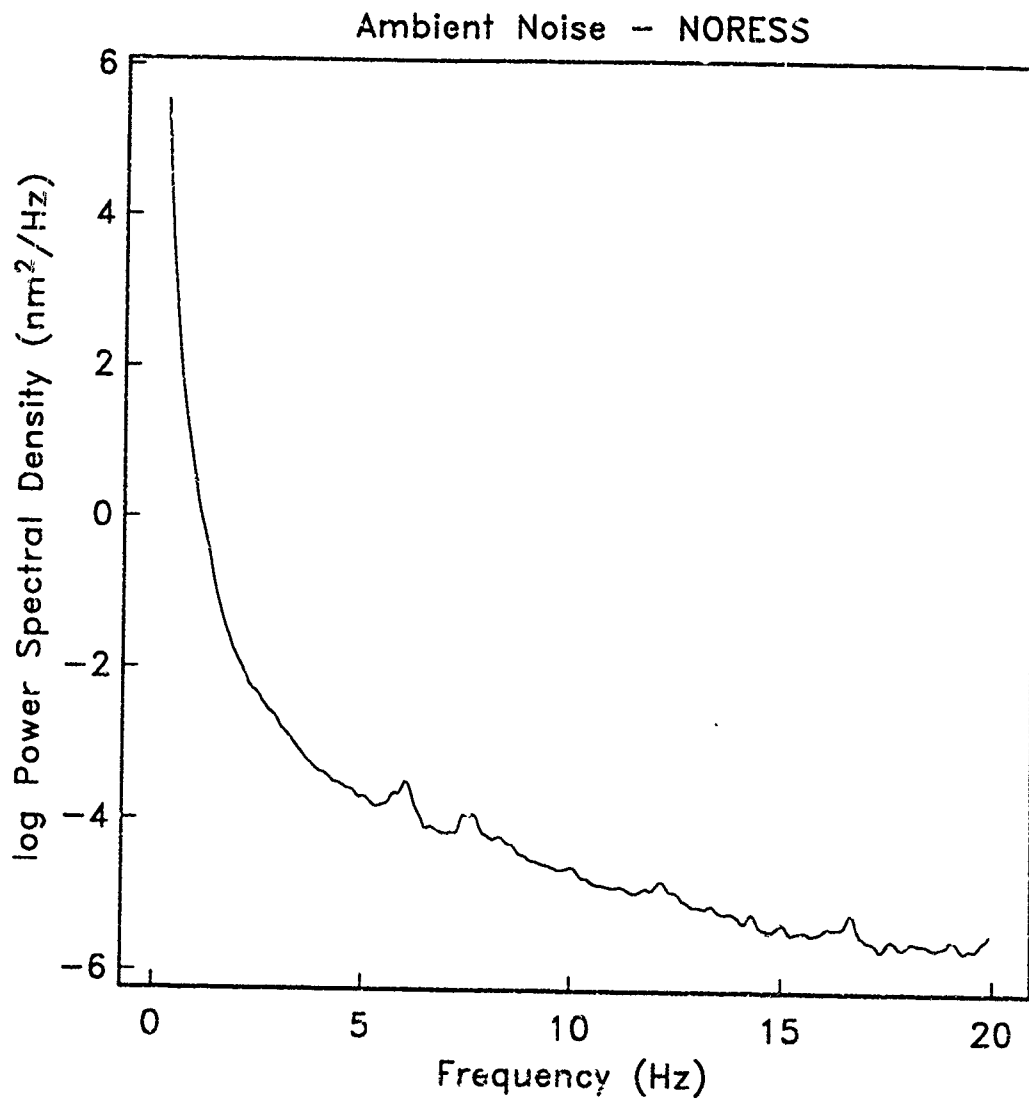


**Figure 4.5.** Input ambient noise power spectral density. The same ambient noise spectrum is assumed for all stations in the network. This is the average single-channel noise spectrum at NORESS [Suteau-Henson and Bache, 1988]. The ambient noise is stored in a one-dimensional data table called *ambient.no* (Table 4.5).

NETSIM TRANSCRIPTION

NetSim

ENTER CONTROL FILE NAME: firun1.cnt

DO YOU WANT TO CREATE THE .LST FILE? (no) yes  
READING CONTROL FILE : firun1.cnt

REVIEW/MODIFY CONTROL FILE?

- A. Enter New Control File
- B. Review/Modify Control File Data
- C. Write New Control File
- D. Continue Reading Other Data Files
- E. Continue Without Any Data Reviews
- X. EXIT PROGRAM

SELECT ITEM: (D) b

Control File Data Types

- A. Control File Data
- B. Frequency Values
- C. File Names
- X. EXIT TO MAIN MENU

SELECT ITEM: (X) a

Control File Parameters

- A. outpre : Firun1
- B. outdir : ./results
- C. cntdir : ./
- D. runtime : detection
- E. subtype : threshcld
- F. detcrit : (P/3)
- G. locwavs : P
- H. sisetype : mlg
- I. evsize : 3.00000
- J. evmin : 1.00000
- K. evmax : 8.00000
- L. probdet : 0.900000
- M. cutlo : 0.
- N. regdest : 20.0000
- O. probloc : 0.900000
- P. numcarlo : 100
- Q. prctlo : 0.500000
- R. prcthi : 0.900000
- S. depthfix : fixed
- T. eventdepth : 0.
- U. numrunfrq : 1

Select item to change or <CR> to CONTINUE

Control File Data Types

- A. Control File Data
- B. Frequency Values
- C. File Names

COMMENTS

The first display is a prompt for the name of the control file. The user enters "firun1.cnt".

An option is given for creating the output list file. NetSim defaults to "no" indicated in parentheses. The user overrides the default by entering "yes".

The user may now review or modify the contents of the control file, write a new control file, or continue reading the other data files.

The user selects "b" to review/modify control file data.

The frequency values and file names for other data files are separated from the main control file data for display purposes.

The user selects "a" to review/modify the main control file data.

NetSim gives a list of the control file parameters and their current values. Any of these can be modified by selecting the letter to the left of the parameter name.

The user enters <(CR)> = carriage return to continue without any modifications.

NetSim returns to the previous menu.

```

X. EXIT TO MAIN MENU
SELECT ITEM: (X) b
Frequency values
A. runfrq( 1) : 1.00000
Select item to change or (<CR> to CONTINUE)
Control File Data Types
A. Control File Data
B. Frequency Values
C. File Names
X. EXIT TO MAIN MENU
SELECT ITEM: (X) c
Control file names
A. file.epi : euras.epi
B. file.smd : granite.smd
C. file.sgr : granite.sgr
D. file.pmd : stable.pmd
E. file.pgr : stable.pgr
F. file.sta : a20x13.sta
Select item to change or (<CR> to CONTINUE)
Control File Data Types
A. Control File Data
B. Frequency Values
C. File Names
X. EXIT TO MAIN MENU
SELECT ITEM: (X)
REVIEW/MODIFY CONTROL FILE?
A. Enter New Control File
B. Review/Modify Control File Data
C. Write New Control File
D. Continue Reading Other Data Files
E. Continue Without Any Data Reviews
X. EXIT PROGRAM
SELECT ITEM: (D)
CONTROL FILES DIRECTORY : ./
Reading Epicenter File : euras.epi
Reading Source Media File : granite.smd
Reading Source Grid File : granite.sgr
Reading Path Media File : stable.pmd
Reading Path Grid File : stable.pgr
Reading Station File : a20x13.sta
SELECT MENU ITEM
A. Enter New Control File

```

```

The user selects "b" to review/modify frequency values.
NetSim lists the frequencies to use in the calculation (in this
case only one frequency is requested, 1 Hz).

The users enters <(CR)> to continue without modification.
NetSim returns to the previous menu.

The user selects "c" to review/modify file names of input files.
NetSim lists the current input file names.

The users enters <(CR)> to continue without modification.
NetSim returns to the previous menu.

The user enters <(CR)> to accept the default, "x".
NetSim returns to the main control file menu.

The user selects "d" to continue reading the other input
data files.
NetSim prints the current control file directory and the
name of the input data files.

The user may now start over with a new control file,
review/modify the contents of any of the input data files,
write any of the input data files (e.g., after modification),

```

| write any of the input data files (e.g., after modification),

A. ENTER NEW CONTROL FILE

- B. Review/Modify Data Files
- C. Write New Data Files
- D. Continue and Read Table Files
- X. EXIT PROGRAM

SELECT ITEM: (D) b

SELECT DATA FILES TO REVIEW/MODIFY

- A. Review/Modify Control File Data
- B. Review/Modify Epicenter File Data
- C. Review/Modify Source Media File Data
- D. Review/Modify Source Grid File Data
- E. Review/Modify Path Media File Data
- F. Review/Modify Path Grid File Data
- G. Review/Modify Station File Data
- X. EXIT TO MAIN MENU

SELECT ITEM: (X) b

Epicenter File Parameters

- A. numepilat : 7
- B. numepilon : 13
- C. epilat1 : 0.
- D. epilon1 : 0.
- E. epilatdel : 15.0000
- F. epilondel : 15.0000

Select item to change or (<CR> to CONTINUE)

SELECT DATA FILES TO REVIEW/MODIFY

- A. Review/Modify Control File Data
- B. Review/Modify Epicenter File Data
- C. Review/Modify Source Media File Data
- D. Review/Modify Source Grid File Data
- E. Review/Modify Path Media File Data
- F. Review/Modify Path Grid File Data
- G. Review/Modify Station File Data
- X. EXIT TO MAIN MENU

SELECT ITEM: (X)

SELECT MENU ITEM

- A. Enter New Control File
- B. Review/Modify Data Files
- C. Write New Data Files
- D. Continue and Read Table Files
- X. EXIT PROGRAM

SELECT ITEM: (D)

TRANSLATING DETECTION CRITERIA

pr((p/3))  
 pr(p/3)

or continue to read data tables.

The user selects "b" to review/modify the input data files.  
 NetSim returns a choice of input data files that can be reviewed/modified.

The user selects "b" to review/modify the epicenter file.  
 NetSim displays the parameters in the epicenter file and their current values.

The user enters <(CR)> to continue without modification.  
 NetSim returns to the previous menu.

The user enters <(CR)> to accept the default, "x".  
 NetSim returns to the main select menu.

The users selects the default "d" to continue and read the data tables.  
 NetSim translates the detection criteria (Ciervo et al., 1985).





0.0000	30.0000	16 Y	8.0000	0.3788
15.0000	30.0000	5 n	7.0109	0.8991
30.0000	30.0000	7 n	5.7309	0.9000
45.0000	30.0000	7 n	4.6503	0.9000
60.0000	30.0000	10 n	4.0459	0.8993
75.0000	30.0000	6 n	4.1916	0.9009
90.0000	30.0000	5 n	4.8553	0.8996
epilat	epsilon	numiter	epsilon	net prob
0.0000	45.0000	14 Y	8.0000	0.8910
15.0000	45.0000	8 n	6.3133	0.9007
30.0000	45.0000	10 n	4.6725	0.9001
45.0000	45.0000	7 n	3.8920	0.9001
60.0000	45.0000	7 n	3.9775	0.9002
75.0000	45.0000	5 n	3.9493	0.8998
90.0000	45.0000	10 n	4.8561	0.9001
epilat	epsilon	numiter	epsilon	net prob
0.0000	60.0000	7 n	7.8278	0.9000
15.0000	60.0000	7 n	6.3320	0.9000
30.0000	60.0000	11 n	4.5649	0.9009
45.0000	60.0000	7 n	3.8022	0.9001
60.0000	60.0000	6 n	5.7066	0.9002
75.0000	60.0000	6 n	3.8783	0.9003
90.0000	60.0000	6 n	4.8558	0.8999
epilat	epsilon	numiter	epsilon	net prob
0.0000	75.0000	5 n	7.7776	0.8998
15.0000	75.0000	7 n	6.1234	0.8996
30.0000	75.0000	8 n	4.6154	0.8993
45.0000	75.0000	7 n	3.9966	0.8993
60.0000	75.0000	4 n	3.6983	0.9000
75.0000	75.0000	6 n	3.8582	0.9001
90.0000	75.0000	7 n	4.8562	0.9002
epilat	epsilon	numiter	epsilon	net prob
0.0000	90.0000	5 n	7.7448	0.8999
15.0000	90.0000	7 n	6.5824	0.8994
30.0000	90.0000	7 n	5.3798	0.9000
45.0000	90.0000	7 n	4.2763	0.8998
60.0000	90.0000	7 n	3.7308	0.8993
75.0000	90.0000	6 n	3.8630	0.9000
90.0000	90.0000	7 n	4.8561	0.9001
epilat	epsilon	numiter	epsilon	net prob
0.0000	105.0000	14 Y	8.0000	0.5192
15.0000	105.0000	5 n	6.9829	0.8998
30.0000	105.0000	7 n	5.5310	0.8992
45.0000	105.0000	7 n	4.4497	0.8999
60.0000	105.0000	7 n	3.7226	0.9000
75.0000	105.0000	7 n	3.9190	0.8999
90.0000	105.0000	9 n	4.8563	0.9002
epilat	epsilon	numiter	epsilon	net prob
0.0000	120.0000	17 Y	8.0000	0.8222

15.0000	120.0000	6 n	6.6668	0.8999
30.0000	120.0000	7 n	5.3865	0.9000
45.0000	120.0000	7 n	4.2682	0.8999
60.0000	120.0000	7 n	3.6733	0.8999
75.0000	120.0000	7 n	4.0081	0.8998
90.0000	120.0000	7 n	4.8573	0.9009
epilat	epsilon	numiter	episize	net prob
0.0000	135.0000	17 Y	8.0000	0.2431
15.0000	135.0000	7 n	7.2419	0.9000
30.0000	135.0000	6 n	5.5833	0.9010
45.0000	135.0000	9 n	4.1972	0.9001
60.0000	135.0000	4 n	3.8725	0.9003
75.0000	135.0000	9 n	4.0787	0.9002
90.0000	135.0000	6 n	4.8564	0.9003
epilat	epsilon	numiter	episize	net prob
0.0000	150.0000	16 Y	8.0000	0.0904
15.0000	150.0000	7 n	7.3824	0.8999
30.0000	150.0000	6 n	6.1065	0.9000
45.0000	150.0000	11 n	4.4205	0.9007
60.0000	150.0000	7 n	3.7908	0.8939
75.0000	150.0000	6 n	4.1047	0.9002
90.0000	150.0000	5 n	4.8546	0.8991
epilat	epsilon	numiter	episize	net prob
0.0000	165.0000	16 Y	8.0000	0.0061
15.0000	165.0000	9 n	7.9414	0.9000
30.0000	165.0000	7 n	6.4444	0.9000
45.0000	165.0000	7 n	5.1805	0.8999
60.0000	165.0000	6 n	4.0311	0.9009
75.0000	165.0000	6 n	4.1116	0.9002
90.0000	165.0000	5 n	4.8551	0.8995
epilat	epsilon	numiter	episize	net prob
0.0000	180.0000	11 Y	8.0000	0.0000
15.0000	180.0000	16 Y	8.0000	0.2424
30.0000	180.0000	6 n	7.0644	0.8997
45.0000	180.0000	7 n	5.5550	0.8990
60.0000	180.0000	14 n	4.0650	0.9001
75.0000	180.0000	7 n	4.1634	0.9000
90.0000	180.0000	5 n	4.8558	0.8999

NetSim offers another run. The user selects the default "no" by entering a <(CR)>.

DO YOU WANT TO MAKE ANOTHER RUN? (no)

## OUTPUT DATA

*NetSim* writes two output data files; the graphics file (*.gra*) and the list file (*.lst*). The formats of these files are described in detail in Appendix A. The graphics file from the sample *NetSim* run is given in Table 4.6. This includes the data in the control file and the data needed to make contour plots (station names and coordinates, detection thresholds, probabilities, and location uncertainties). The last nine columns of the matrix in Table 4.6 are zero because these are location uncertainties and the sample *NetSim* run only calculated detection thresholds. Table 4.7 lists the first three pages of the list file, and one page for epicenter 33 (there is one page of detection parameters for each epicenter).

## SNAPCON TRANSCRIPTION

A complete transcription of an interactive *SnapCon* session to generate a contour map of the detection thresholds calculated in the sample *NetSim* run starts on page 46 of this report. Comments are separated from the transcription by a vertical line on each page. This transcription is included as an example of the *SnapCon* user-interface.

OUTPUT GRAPHICS FILE: ./results/Firun1.gra

```

Title of Run
Date and Time of Run
Control File Name
Epicenter File Name
Source Media File Name
Path Grid File Name
Path Grid File Name
Station File Name
Output Prefix
Output Directory
Input Directory
Run Type
Sub-run Type
Detection Criteria
Waves to Use in Location
Event Size Type
Event Size
Minimum Event Size
Maximum Event Size
Probability of Detection
Low Probability Cutoff
Regional Distance
Location Confidence Level
Number of Monte Carlo Simulations
Low & Monte Carlo
High & Monte Carlo
Fixed or Free Depth
Event Depth
Number of Frequencies
Run Frequencies
: Frequency-Independent Detection Thresholds
: 03-01-90 13:09
: firun1.cnt
: euras.epi
: granite.smd
: granite.sgr
: stable.pmd
: stable.pgr
: a20x13.sta
: Firun1
: ./results
: ./
: detection
: threshold
: (P/3)
: P
: mlg
: 3.000
: 1.000
: 8.000
: 0.900
: 0.000
: 20.000
: 0.900
: 100
: 0.500
: 0.900
: fixed
: 0.000
: 1
: 1.000
6.0735E+01 1.1542E+01
2.5567E+01 9.1983E+01
3.0188E+01 6.6950E+01
6.9250E+01-5.3533E+01
6.2480E+01-1.1459E+02
3.9900E+01 3.2783E+01
1.4662E+01 1.2108E+02
3.6542E+01 1.3821E+02
7.1303E+01-1.5675E+02
3.9881E+01-4.0490E+00
6.1592E+01-1.4913E+02
5.8762E+01-9.4087E+01
7.0500E+01 2.7000E+01
5.0000E+01 1.1100E+02
6.4900E+01-1.7200E+02
5.0000E+01 1.4300E+02
3.5000E+01 5.7000E+01
4.5000E+01 5.9900E+01
4.5000E+01 7.4800E+01
4.5000E+01 4.4900E+01
5.5000E+01 4.8900E+01
5.5000E+01 6.7800E+01
5.5000E+01 8.6700E+01
5.5000E+01 1.0560E+02
5.5000E+01 1.2450E+02
33
NOR
SHIO
GUPO
GDH
RSTN
ANTO
MAN
MAJO
BRW
TOL
PMR
FCC
NR2
S1
S2
S3
S5
S6
S7
S8
S9
S10
S11
S12
S13

```

Table 4.6. Sample output graphics file.





OUTPUT LIST FILE: ./results/Firun1.lst (page 1)

```

Title of Run      : Frequency-Independent Detection Thresholds
Date and Time of Run : 03-01-90 13:09
Control File Name  : firun1.cnt
Epicenter File Name : auras.epi
Source Media File Name : granite.smd
Source Grid File Name : granite.sgr
Path Media File Name : stable.pmd
Path Grid File Name : stable.pgr
Station File Name : a20x13.sta
Output Prefix      : Firun1
Output Directory   : ./results
Input Directory     : ./
Run Type           : detection
Sub-run Type       : threshold
Detection Criteria : (P/3)
Waves to Use in Location : P
Event Size Type    : mlg
Event Size         : 3.000
Minimum Event Size : 1.000
Maximum Event Size : 8.000
Probability of Detection : 0.900
Low Probability Cutoff : 0.000
Regional Distance  : 20.000
Location Confidence Level : 0.900
Number of Monte Carlo Simulations : 100
Low & Monte Carlo  : 0.500
High & Monte Carlo : 0.900
Fixed or Free Depth : fixed
Event Depth        : 0.000
Number of Frequencies : 1
Run Frequencies    : 1.000

```

Table 4.7. Sample output list file.

STATION DATA

STATION FILE DIRECTORY: ./station

I	IDENT	LAT.	LONG.	RELIAB.	DENSITY	NOISE SD	AMBIENT-NOISE TABLE
1	NOR	60.735	11.542	1.000	2500.000	0.100	ambient.noi
2	SHIO	25.567	91.883	1.000	2500.000	0.100	ambient.noi
3	GUPO	30.188	66.950	1.000	2500.000	0.100	ambient.noi
4	GDUH	69.250	-53.533	1.000	2500.000	0.100	ambient.noi
5	RSTW	62.480	-114.592	1.000	2500.000	0.100	ambient.noi
6	ANTO	39.900	32.783	1.000	2500.000	0.100	ambient.noi
7	KAN	14.662	121.077	1.000	2500.000	0.100	ambient.noi
8	MAJO	36.542	138.209	1.000	2500.000	0.100	ambient.noi
9	BNW	71.303	-156.748	1.000	2500.000	0.100	ambient.noi
10	TOL	39.881	-4.049	1.000	2500.000	0.100	ambient.noi
11	PMR	61.592	-149.131	1.000	2500.000	0.100	ambient.noi
12	FCC	58.762	-94.087	1.000	2500.000	0.100	ambient.noi
13	NR2	70.500	27.000	1.000	2500.000	0.100	ambient.noi
14	S1	50.000	111.000	1.000	2500.000	0.100	ambient.noi
15	S2	64.900	-172.000	1.000	2500.000	0.100	ambient.noi
16	S3	50.000	143.000	1.000	2500.000	0.100	ambient.noi
17	S5	35.000	57.000	1.000	2500.000	0.100	ambient.noi
18	S6	45.000	59.900	1.000	2500.000	0.100	ambient.noi
19	S7	45.000	74.800	1.000	2500.000	0.100	ambient.noi
20	S8	45.000	44.900	1.000	2500.000	0.100	ambient.noi
21	S9	55.000	48.900	1.000	2500.000	0.100	ambient.noi
22	S10	55.000	67.800	1.000	2500.000	0.100	ambient.noi
23	S11	55.000	86.700	1.000	2500.000	0.100	ambient.noi
24	S12	55.000	105.600	1.000	2500.000	0.100	ambient.noi
25	S13	55.000	124.500	1.000	2500.000	0.100	ambient.noi
26	S14	54.900	160.000	1.000	2500.000	0.100	ambient.noi
27	S15	65.000	55.000	1.000	2500.000	0.100	ambient.noi
28	S16	65.000	81.600	1.000	2500.000	0.100	ambient.noi
29	S17	65.000	108.200	1.000	2500.000	0.100	ambient.noi
30	S18	65.000	134.800	1.000	2500.000	0.100	ambient.noi
31	S19	65.000	161.400	1.000	2500.000	0.100	ambient.noi
32	S20	76.500	67.000	1.000	2500.000	0.100	ambient.noi
33	S21	77.500	105.100	1.000	2500.000	0.100	ambient.noi

Table 4.7. Sample output list file (continued).

OUTPUT LIST FILE: ./results/Firun1.lst (page 3)

STATION TABLE (P -WAVE)

I	IDENT	STATION CORRECTION	S/N RATIO	WAVE VELOCITY	SIGNAL SD	TIME SD	AZIMUTH		SITE-RESPONSE TABLE	
							SD	SD	SD	SD
1	NOR	0.000	4.000	5000.000	0.000	0.000	0.000	0.000	0.000	ARRAY.SIS
2	SHIO	0.000	4.000	5000.000	0.000	0.000	0.000	0.000	0.000	ARRAY.SIS
3	GUPO	0.000	4.000	5000.000	0.000	0.000	0.000	0.000	0.000	ARRAY.SIS
4	GDPH	0.000	4.000	5000.000	0.000	0.000	0.000	0.000	0.000	ARRAY.SIS
5	RSTN	0.000	4.000	5000.000	0.000	0.000	0.000	0.000	0.000	ARRAY.SIS
6	ANTO	0.000	4.000	5000.000	0.000	0.000	0.000	0.000	0.000	ARRAY.SIS
7	MAN	0.000	4.000	5000.000	0.000	0.000	0.000	0.000	0.000	ARRAY.SIS
8	MAJO	0.000	4.000	5000.000	0.000	0.000	0.000	0.000	0.000	ARRAY.SIS
9	BRW	0.000	4.000	5000.000	0.000	0.000	0.000	0.000	0.000	ARRAY.SIS
10	TOL	0.000	4.000	5000.000	0.000	0.000	0.000	0.000	0.000	ARRAY.SIS
11	PMR	0.000	4.000	5000.000	0.000	0.000	0.000	0.000	0.000	ARRAY.SIS
12	FCC	0.000	4.000	5000.000	0.000	0.000	0.000	0.000	0.000	ARRAY.SIS
13	MR2	0.000	4.000	5000.000	0.000	0.000	0.000	0.000	0.000	ARRAY.SIS
14	S1	0.000	4.000	5000.000	0.000	0.000	0.000	0.000	0.000	ARRAY.SIS
15	S2	0.000	4.000	5000.000	0.000	0.000	0.000	0.000	0.000	ARRAY.SIS
16	S3	0.000	4.000	5000.000	0.000	0.000	0.000	0.000	0.000	ARRAY.SIS
17	S5	0.000	4.000	5000.000	0.000	0.000	0.000	0.000	0.000	ARRAY.SIS
18	S6	0.000	4.000	5000.000	0.000	0.000	0.000	0.000	0.000	ARRAY.SIS
19	S7	0.000	4.000	5000.000	0.000	0.000	0.000	0.000	0.000	ARRAY.SIS
20	S8	0.000	4.000	5000.000	0.000	0.000	0.000	0.000	0.000	ARRAY.SIS
21	S9	0.000	4.000	5000.000	0.000	0.000	0.000	0.000	0.000	ARRAY.SIS
22	S10	0.000	4.000	5000.000	0.000	0.000	0.000	0.000	0.000	ARRAY.SIS
23	S11	0.000	4.000	5000.000	0.000	0.000	0.000	0.000	0.000	ARRAY.SIS
24	S12	0.000	4.000	5000.000	0.000	0.000	0.000	0.000	0.000	ARRAY.SIS
25	S13	0.000	4.000	5000.000	0.000	0.000	0.000	0.000	0.000	ARRAY.SIS
26	S14	0.000	4.000	5000.000	0.000	0.000	0.000	0.000	0.000	ARRAY.SIS
27	S15	0.000	4.000	5000.000	0.000	0.000	0.000	0.000	0.000	ARRAY.SIS
28	S16	0.000	4.000	5000.000	0.000	0.000	0.000	0.000	0.000	ARRAY.SIS
29	S17	0.000	4.000	5000.000	0.000	0.000	0.000	0.000	0.000	ARRAY.SIS
30	S18	0.000	4.000	5000.000	0.000	0.000	0.000	0.000	0.000	ARRAY.SIS
31	S19	0.000	4.000	5000.000	0.000	0.000	0.000	0.000	0.000	ARRAY.SIS
32	S20	0.000	4.000	5000.000	0.000	0.000	0.000	0.000	0.000	ARRAY.SIS
33	S21	0.000	4.000	5000.000	0.000	0.000	0.000	0.000	0.000	ARRAY.SIS

Table 4.7. Sample output list file (continued).

OUTPUT LIST FILE: ./results/Firun1.lst (page X)

EPICENTER 33 LAT= 60.000 LONG= 60.000  
 EVENT SIZE : 3.707 NETWORK PROBABILITY (%) : 90.018  
 NUMBER OF ITERATIONS : 6 ITERATION BOUNDS EXCEEDED :  
 SEMI-MAJOR AXIS (LO) : 1.000 SEMI-MAJOR AXIS (HI) : 0.000  
 SEMI-MINOR AXIS (LO) : 0.000 SEMI-MINOR AXIS (HI) : 0.000  
 STRIKE (LO) : 0.000 STRIKE (HI) : 0.000  
 DEPTH-INTERVAL (LO) : 0.000 DEPTH-INTERVAL (HI) : 0.000  
 MONTE CARLO FRACTION : 0.000

STATION	ANG. DIST.	AZM	STATION PROB.	F -WAVE FREQ. MAX.	OF AMPL. S/N	ATTEN. SD
1 NOR	23.424	293.015	0.000	1.000	0.300	0.300
2 SHIO	40.822	133.209	0.000	1.000	0.300	0.300
3 GUPO	30.776	167.990	0.000	1.000	0.300	0.300
4 GDX	42.343	331.168	0.000	1.000	0.300	0.300
5 RSTN	57.450	357.039	0.000	1.000	0.300	0.300
6 ANTO	26.282	232.411	0.000	1.000	0.300	0.300
7 MAN	63.054	108.215	0.000	1.000	0.300	0.300
8 MAJO	53.293	78.814	0.000	1.000	0.300	0.300
9 ZRW	46.220	15.405	0.000	1.000	0.300	0.300
10 TOL	43.681	272.471	0.000	1.000	0.300	0.300
11 PMR	56.361	16.152	0.000	1.000	0.300	0.300
12 FCC	59.520	344.754	0.000	1.000	0.300	0.300
13 NR2	16.995	321.538	0.018	1.000	0.300	0.300
14 S1	30.040	86.255	0.000	1.000	0.300	0.300
15 S2	49.182	26.213	0.000	1.000	0.300	0.300
16 S3	45.365	63.710	0.000	1.000	0.300	0.300
17 S5	25.076	185.806	0.000	1.000	0.300	0.300
18 S6	15.000	180.273	0.068	1.000	0.300	0.300
19 S7	17.408	142.862	0.013	1.000	0.300	0.300
20 S8	17.500	217.777	0.012	1.000	0.300	0.300
21 S9	7.765	234.812	0.857	1.000	0.300	0.300
22 S10	6.515	136.684	0.948	1.000	0.300	0.300
23 S11	15.069	97.557	0.065	1.000	0.300	0.300
24 S12	24.486	81.393	0.000	1.000	0.300	0.300
25 S13	33.605	69.290	0.000	1.000	0.300	0.300
26 S14	48.806	48.811	0.000	1.000	0.300	0.300
27 S15	5.503	337.414	0.983	1.000	0.300	0.300
28 S16	11.081	54.042	0.421	1.000	0.300	0.300
29 S17	22.221	56.415	0.000	1.000	0.300	0.300
30 S18	32.829	48.787	0.000	1.000	0.300	0.300
31 S19	42.002	38.251	0.000	1.000	0.300	0.300
32 S20	16.675	5.690	0.023	1.000	0.300	0.300
33 S21	22.797	23.309	0.000	1.000	0.300	0.300

Table 4.7. Sample output list file (continued).

SNAPCON TRANSCRIPTION

\* SnapCon

MAIN MENU

- S - Read Single Data File
- D - Read Difference 2 Data Files
- E - Read Compute Percent Change Between 2 Files
- G - Read File Group/Interpolate Mag at Fixed Loc Error
- F - Change Simulation Parameter Using Active File(s)
- V - Update Plot Options
- C - Compose and Store Contour Plot
- Q - Quit

?\_s  
Data File?\_ Firun1.gra

SIMULATION PARAMETER MENU

1 = Magnitude Thresholds / Probability of Detection

Location Uncertainties:

- 2 = Semi-Major Axis
- 3 = Semi-Minor Axis
- 4 = Depth
- 5 = Area of Ellipse
- 6 = Equivalent Circle Radius

?\_1

PLOT OPTIONS MENU

- A - Projection [Cylindrical Equidistant ]
- B - Longitude [ 0.0, 180.0]
- C - Latitude [ 0.0, 90.0]
- D - Contour Options [default=Y]
- E - Plot Stations, names? [plot contours=Y]
- F - Plot Coastlines, Dotted? [Y,Y]
- G - Plot Grid Lines? [N]
- H - Title? [ ]
- I - Classification? [none]
- Q - Exit This Menu

?\_c  
Latitude limits?\_ 30 90

PLOT OPTIONS MENU

- A - Projection [Cylindrical Equidistant ]
- B - Longitude [ 0.0, 180.0]
- C - Latitude [ 30.0, 90.0]
- D - Contour Options [default=Y]
- E - Plot Stations, names? [plot contours=Y]
- F - Plot Coastlines, Dotted? [Y,Y]
- G - Plot Grid Lines? [N]
- H - Title? [ ]
- I - Classification? [none]
- Q - Exit This Menu

?\_d

CONTOUR OPTION? MENU

COMMENTS

SnapCon begins with a main menu prompt. The various options are described in Section 3.3.

The user selects "s" for read single data file. SnapCon prompts for the file name, and the user enters the name of the output graphics file, "firun1.gra".

The user may now select detection (threshold or probability) or location parameters to display as contours on a map.

The user selects option "1", Magnitude Thresholds/Probability of Detection.

SnapCon lists a menu of plot options and current values. The user can change any of the current values by entering the letter to left of the menu item.

The user selects "c" to change the latitude limits. SnapCon prompts for new limits, and the user enters "30 90".

SnapCon returns to the plot options menu.

The user selects "d" to modify contour options.

The user selects "d" to modify contour options.

CONTOUR OPTION? MENU

SnapCon lists the contour options menu and current parameter values.

A - Contour Interval?  
B - Contour Limits?  
C - Plot Contours?  
D - Default Tension?  
Q - Exit This Menu

[ 0.00 ]  
[ 3.6733 , 8.0000 ]  
[ Y ]  
[ Y, tension= 2.5 ]

The user selects "a" to fix the contour interval. SnapCon prompts for the new interval, and the user enters "0.2".

? \_ a  
Contour interval?\_ 0.2

SnapCon returns to the contour options menu.

CONTOUR OPTIONS MENU

A - Contour Interval?  
B - Contour Limits?  
C - Plot Contours?  
D - Default Tension?  
Q - Exit This Menu

[ 0.20 ]  
[ 3.6733 , 8.0000 ]  
[ Y ]  
[ Y, tension= 2.5 ]

The user selects "b" to change the contour limits. SnapCon prompts for the new limits, and the user enters "3.6 6.0".

? \_ b  
Contour minimum and maximum?\_ 3.6 6.0

SnapCon returns to the contour options menu.

CONTOUR OPTIONS MENU

A - Contour Interval?  
B - Contour Limits?  
C - Plot Contours?  
D - Default Tension?  
Q - Exit This Menu

[ 0.20 ]  
[ 3.6000 , 6.0000 ]  
[ Y ]  
[ Y, tension= 2.5 ]

The user selects "q" to exit this menu.

? \_ q

SnapCon returns to the plot options menu.

PLOT OPTIONS MENU

A - Projection  
B - Longitude  
C - Latitude  
D - Contour Options  
E - Plot Stations, names?  
F - Plot Coastlines, Dotted?  
G - Plot Grid Lines?  
H - Title?  
I - Classification?  
Q - Exit This Menu

[Cylindrical Equidistant ]  
[ 0.0, 180.0 ]  
[ 30.0, 90.0 ]  
[default=N]  
[plot contours=Y]  
[Y,Y]  
[Y,Y]  
[N]  
[ ]  
[none]

The user enters "h" to change the title of the plot. SnapCon prompts for a new title, and the user enters "FREQ-INDEP DETECTION THRESHOLDS (1 HZ)".

? \_ h  
Title for Plot? (must be in all caps)  
FREQ-INDEP DETECTION THRESHOLDS (1 HZ)

SnapCon returns to the plot options menu.

PLOT OPTIONS MENU

A - Projection  
B - Longitude  
C - Latitude  
D - Contour Options  
E - Plot Stations, names?  
F - Plot Coastlines, Dotted?  
G - Plot Grid Lines?  
H - Title?  
I - Classification?  
Q - Exit This Menu

[Cylindrical Equidistant ]  
[ 0.0, 180.0 ]  
[ 30.0, 90.0 ]  
[default=N]  
[plot contours=Y]  
[Y,Y]  
[Y,Y]  
[N]  
[FREQ-INDEP DETECTION THRESHOLDS (1 HZ)]  
[none]

The user selects "q" to exit this menu.

? \_ q

SnapCon returns to the main menu.

MAIN MENU

?\_o  
S - Read Single Data File  
D - Read Difference 2 Data Files  
P - Read Compute Percent Change Between 2 Files  
G - Read File Group/Interpolate Mag at Fixed Loc Error  
T - Change Simulation Parameter Using Active File(s)  
U - Update Plot Options  
C - Compose and Store Contour Plot  
Q - Quit

UMIN = -90.000000 UMAX = 90.000000  
VMIN = 30.000000 VMAX = 90.000000

MAIN MENU

?\_q  
S - Read Single Data File  
D - Read Difference 2 Data Files  
P - Read Compute Percent Change Between 2 Files  
G - Read File Group/Interpolate Mag at Fixed Loc Error  
T - Change Simulation Parameter Using Active File(s)  
U - Update Plot Options  
C - Compose and Store Contour Plot  
Q - Quit

---  
To make a laser printer plot, use the command:  
"mctrplot1 snapcon.met | pplot |lpr"  
For multiple plots in the same plotfile you must  
hit a carriage return for each plot.

To plot on the sun console, use the command:  
"mctrsun snapcon.met "

-----  
The user selects "c" to compose and store plot.  
SnapCon creates a metacode file called "snapcon.met"

SnapCon returns to the main menu.

-----  
The user selects "q" to end this SnapCon session.  
SnapCon informs the user how to send the metacode file  
to various output devices.

## DETECTION THRESHOLDS

Figure 4.6a plots contours of the detection thresholds calculated for the *NetSim* sample run at 1.0 Hz (this is the result of the *SnapCon* session described above). The detection threshold is *MLg* 3.7–4.2 for epicenters in the Soviet Union. Figure 4.6b plots the detection thresholds at 10 Hz. These results were obtained by changing the frequency in the control file (Table 4.1) to 10 Hz, and repeating the *NetSim* calculations described for the first sample run. The 90% *MLg* threshold for detecting 3 *P* waves at 10 Hz is 2.8–5.3 for epicenters in the Soviet Union. The threshold at 10 Hz is lower than the threshold at 1 Hz for epicenters in areas with dense station coverage, but the threshold is much higher at 10 Hz than at 1 Hz for epicenters in areas with sparse station coverage. This is because the frequency of the maximum signal-to-noise ratio (SNR) decreases with increasing epicentral distance. It is clear from these examples that frequency dependent input parameters are required to obtain accurate estimates of detection capability at regional distances.

### 4.2 Frequency-Dependent Input

This section presents the results of a sample *NetSim* run that includes frequency dependence in the source, attenuation, station noise, and beam gain. We use the same input data files that were described in Section 4.1, except that we have modified the control file to include 11 frequencies between 1.0 and 20.0 Hz (Table 4.8). The results of the calculation are plotted in Figure 4.7. The frequency-dependent 90% *MLg* threshold for detecting 3 *P* waves is 2.6–3.4 for epicenters in the Soviet Union. These thresholds are less than the thresholds for either 1 Hz or 10 Hz (Figure 4.6). This is because the frequency of the maximum SNR is greater than 1 Hz and less than 10 Hz for epicentral distances important for determining the detection threshold for the network. For example, Figure 4.8 plots the frequency of the maximum SNR as function of epicentral distance for an epicenter in western USSR (60° N, 60° E). Table 4.9 lists the detection parameters for this epicenter. The frequency of the maximum SNR is 4–7 Hz for all stations that have a probability of detection greater than zero.

### 4.3 Probability-Weighted and Monte Carlo Location

There are two ways that *NetSim* can account for the effect of undetected phases on location uncertainties; the probability-weighted approach (used in *SNAP/D*) and the Monte Carlo approach described in Section 2.3.2. In this section we compare the location uncertainties computed using these two methods for events near the 3 *P* detection threshold of the network. We also compare the two approaches for one epicenter in western USSR as a function of event size.

We use the same input data files for our location uncertainty simulations that we used for our detection threshold simulations (Section 4.3). The only difference is the *runtyp* parameter in the control file in Table 4.8 was changed to *detloc* to compute the median and 90th percentile Monte Carlo location uncertainties. The probability-weighted

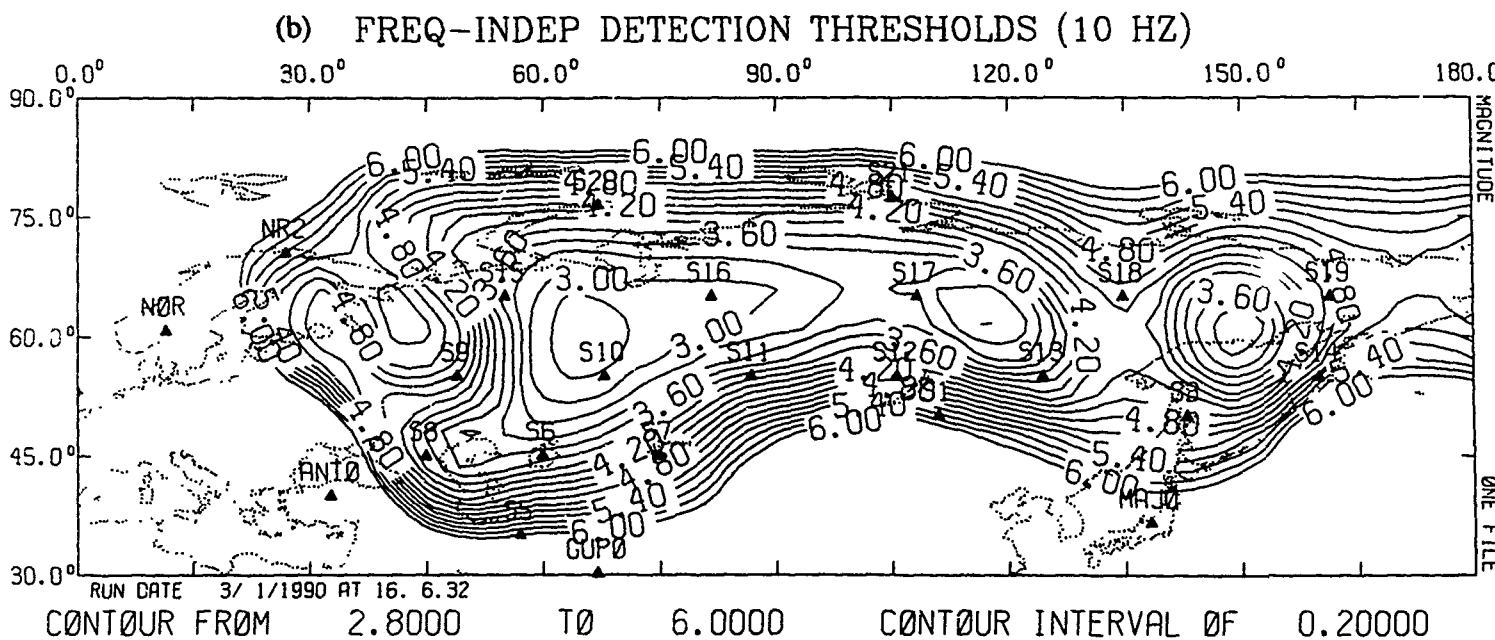
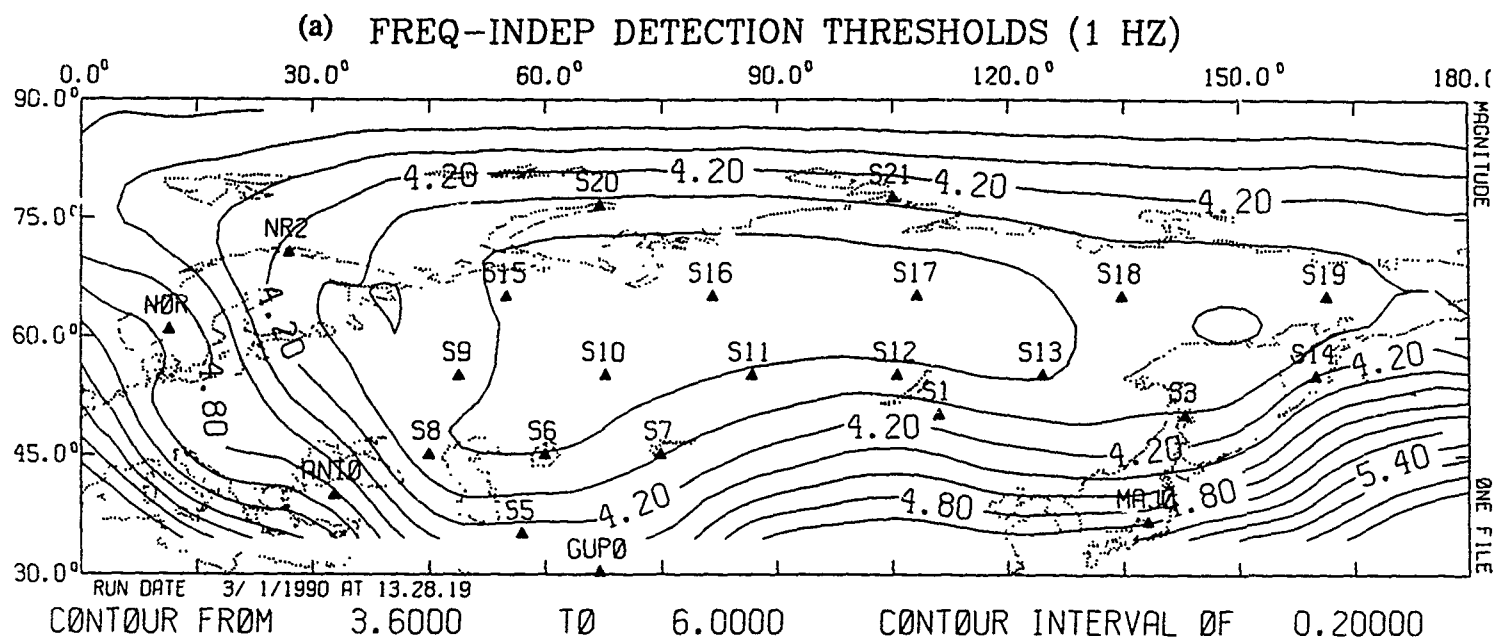


Figure 4.6. Contours of the 90%  $ML_g$  thresholds for detecting 3  $P$  phases at (a) 1 Hz, and (b) 10 Hz.

CONTROL DATA

CONTROL FILE: ./fdrunl.cnt

Frequency-Dependent Detection Thresholds

FDrunl

./results

./

detection

threshold

(P/3)

P

mlg

3.000	1.000	8.000	0.900	0.900	20.000
0.900	100	0.590	0.900		

fixed 0.000

11

1. 2. 3. 4. 5.

6. 7. 8. 10. 15. 20.

euras.epi

granite.smd

granite.sgr

able.pmd

able.pgr

40x13.sta

Table 4.8. Sample control file (frequency-dependent input).

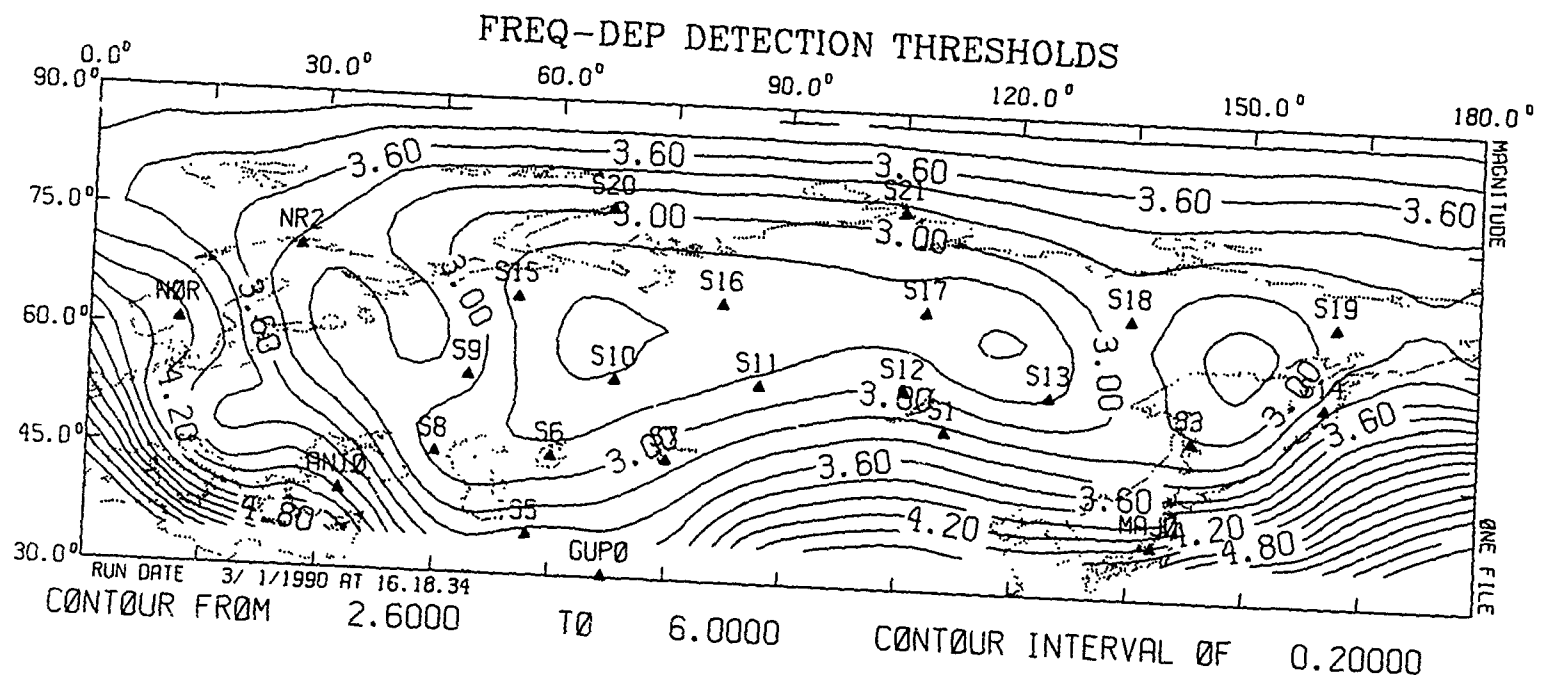
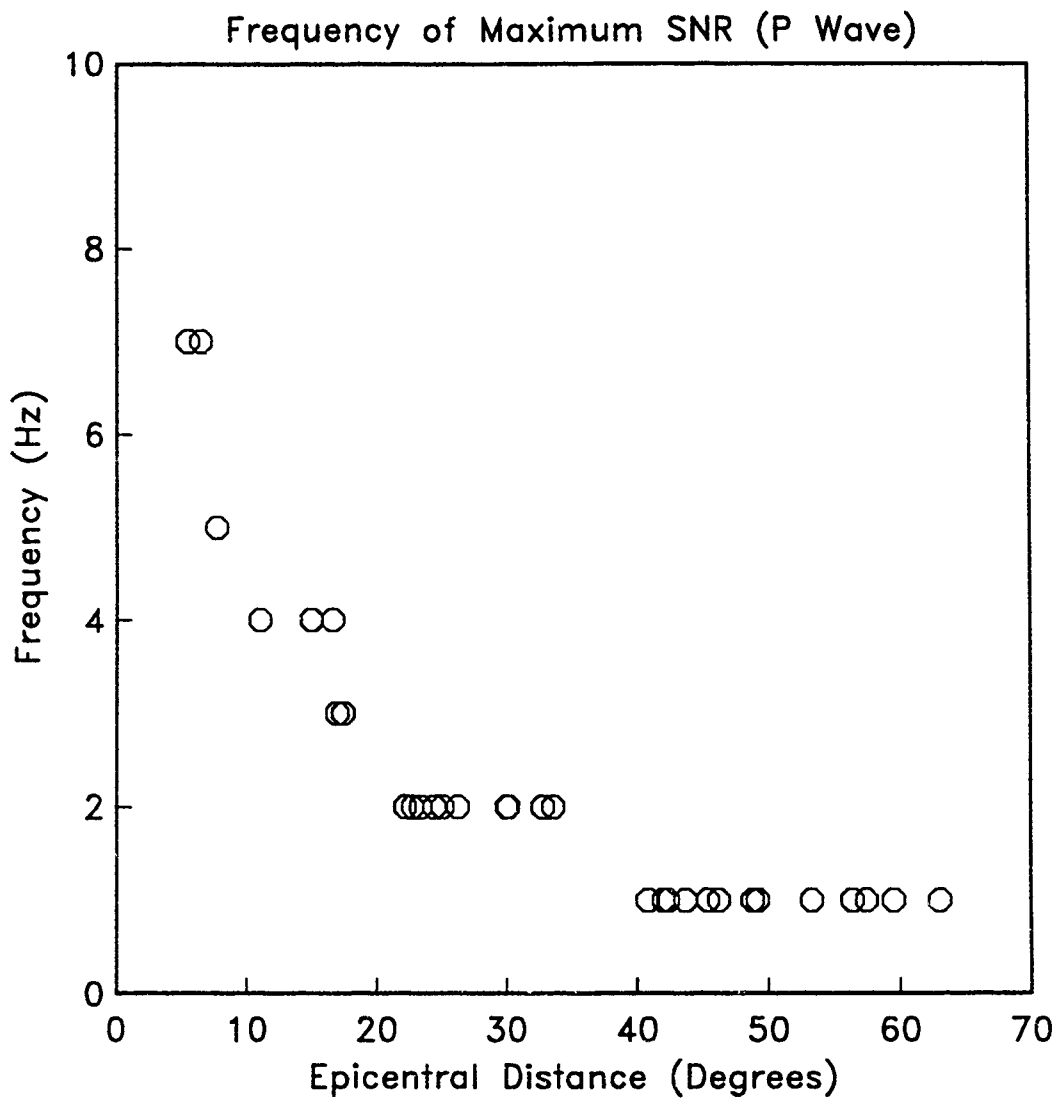


Figure 4.7. Contours of the 90% *MLg* thresholds for detecting 3 *P* phases using broad band (1-20 Hz) input.



**Figure 4.8.** Frequency of the maximum SNR as a function of epicentral distance for *P* phases. This figure plots the values in Table 4.9 for an epicenter in the western USSR ( $60^\circ$  N,  $60^\circ$  E).

OUTPUT LIST FILE: ./results/FDrun1.lst

EPICENTER 33 LAT= 60.000 LONG= 60.000

EVENT SIZE	:	2.598	NETWORK PROBABILITY (%)	:	89.977
NUMBER OF ITERATIONS	:	6	ITERATION BOUNDS EXCEEDED	:	n
SEMI-MAJOR AXIS (LO)	:	0.000	SEMI-MAJOR AXIS (HI)	:	0.000
SEMI-MINOR AXIS (LO)	:	0.000	SEMI-MINOR AXIS (HI)	:	0.000
STRIKE (LO)	:	0.000	STRIKE (HI)	:	0.000
DEPTH-INTERVAL (LO)	:	0.000	DEPTH-INTERVAL (HI)	:	0.000
MONTE CARLO FRACTION	:	0.000		:	

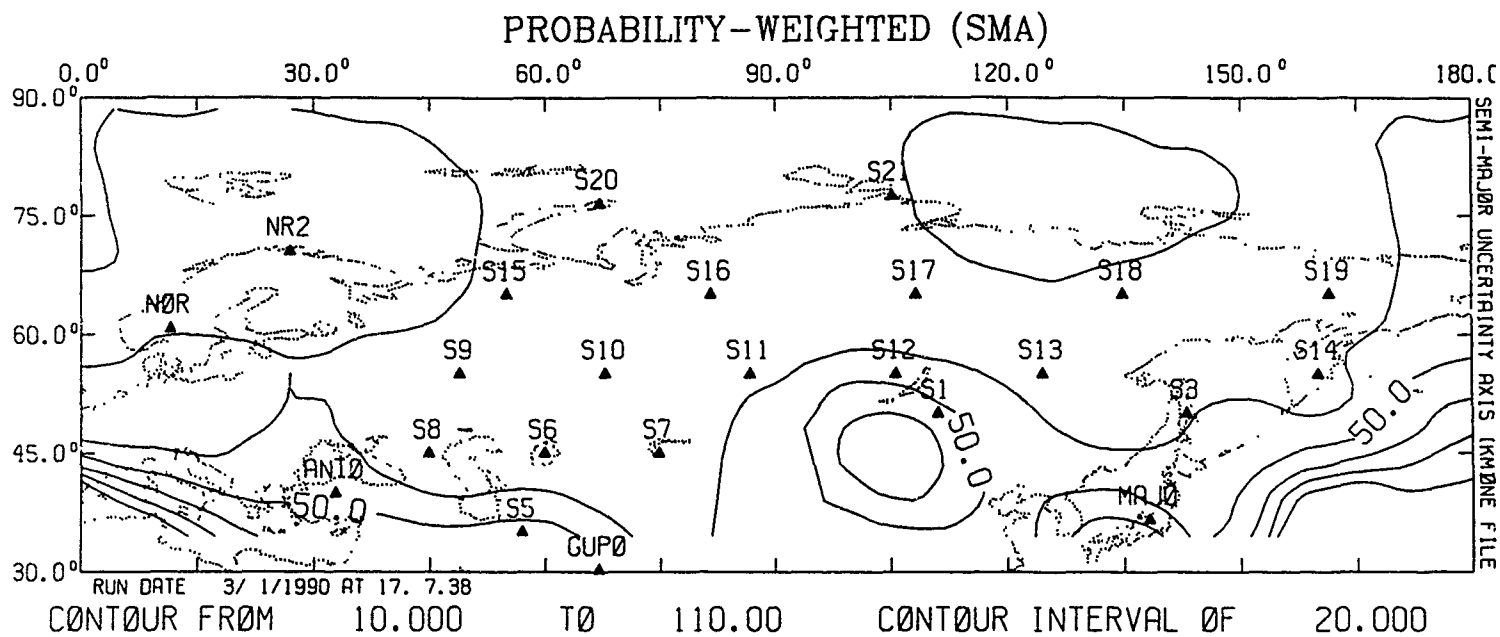
STATION	ANG. DIST.	AZM	STATION PROB.	P -WAVE	
				FREQ. OF MAX. S/N	AMPL. ATTEN.SD
1 NOR	23.424	293.015	0.000	2.000	0.300
2 SHIO	40.822	133.209	0.000	1.000	0.300
3 GUPO	30.175	167.990	0.000	2.000	0.300
4 GDH	42.343	331.168	0.000	1.000	0.300
5 RSTN	57.450	357.039	0.000	1.000	0.300
6 ANTO	26.282	232.411	0.000	2.000	0.300
7 MAN	63.054	108.215	0.000	1.000	0.300
8 MAJO	53.293	78.814	0.000	1.000	0.300
9 BRW	46.220	15.405	0.000	1.000	0.300
10 TOL	43.681	272.471	0.000	1.000	0.300
11 PMR	56.361	16.152	0.000	1.000	0.300
12 FCC	59.520	344.754	0.000	1.000	0.300
13 NR2	16.995	321.538	0.000	3.000	0.300
14 S1	30.040	86.255	0.000	2.000	0.300
15 S2	49.182	26.213	0.000	1.000	0.300
16 S3	45.365	63.710	0.000	1.000	0.300
17 S5	25.076	185.806	0.000	2.000	0.300
18 S6	15.000	180.273	0.002	4.000	0.300
19 S7	17.408	142.862	0.000	3.000	0.300
20 S8	17.500	217.777	0.000	3.000	0.300
21 S9	7.765	234.812	0.888	5.000	0.300
22 S10	6.515	136.684	0.984	7.000	0.300
23 S11	15.069	97.557	0.001	4.000	0.300
24 S12	24.486	81.393	0.000	2.000	0.300
25 S13	33.605	69.290	0.000	2.000	0.300
26 S14	48.806	48.811	0.000	1.000	0.300
27 S15	5.503	337.414	0.999	7.000	0.300
28 S16	11.081	54.042	0.210	4.000	0.300
29 S17	22.221	56.415	0.000	2.000	0.300
30 S18	32.829	48.787	0.000	2.000	0.300
31 S19	42.002	38.251	0.000	1.000	0.300
32 S20	16.675	5.690	0.000	4.000	0.300
33 S21	22.797	23.309	0.000	2.000	0.300

Table 4.9. Sample list file (frequency-dependent input).

location uncertainties were calculated by changing *numcarlo* in the control file to 1 (see Appendix A). Figure 4.9 plots the probability-weighted estimate of the semi-major axis (SMA) of the epicentral error ellipse. The probability-weighted SMA is between 14 and 40 km for epicenters in the Soviet Union. The results for the median and 90th percentile Monte Carlo realizations are plotted in Figure 4.10. The median Monte Carlo SMA is between 13 and 45 km for events in the Soviet Union. This is similar to the range produced by the probability-weighted approach (the average difference between the median Monte Carlo SMA and the probability-weighted SMA is 3.3 km for epicenters in the Soviet Union). The 90th percentile Monte Carlo realization SMA is between 20 and 235 km for events in the Soviet Union, which is significantly larger than the median Monte Carlo SMA or the probability-weighted SMA.

The results in Figures 4.9 and 4.10 are for events at the 90% *MLg* threshold for detecting 3 *P* phases. Since azimuth and arrival time can be estimated for each *P* detection, there should be more than enough data to constrain the event epicenter (assuming fixed depth). We found that at least 95% of the Monte Carlo realizations had enough data to constrain the event epicenters in the Soviet Union. However, we also found that the probability-weighted approach increasingly underestimates the median Monte Carlo SMA as the event magnitude decreases. For example, Figure 4.11 plots histograms of the SMA computed using the Monte Carlo approach for three different event magnitudes at an epicenter in western USSR (60° N, 60° E). One hundred realizations were generated for each magnitude. Figure 4.11a is for *MLg* 3.0, which is greater than the 3 *P* detection threshold at this epicenter. The probability-weighted SMA is nearly equal to the median Monte Carlo SMA (19 km), and less than the 90th percentile Monte Carlo SMA (27 km). Figure 4.11b is for *MLg* 2.58, which is equal to the 3 *P* detection threshold. Again the probability-weighted SMA (25 km) is close to the median Monte Carlo SMA (27 km), but it is substantially less than the 90th percentile Monte Carlo SMA (140 km). Figure 4.11c is for *MLg* 2.23, which is equal to the 2 *P* detection threshold. In this case, only 79% of the Monte Carlo realizations had enough data to constrain the location. The probability-weighted SMA is 34.6 km, while the median and 90th percentile Monte Carlo estimates are both 140 km. It is clear from Figure 4.11 that a decrease in the event magnitude results in an increase in the discrepancy between the probability-weighted and Monte Carlo approaches.

The probability-weighted approach is most accurate when an individual datum is not very important for constraining the location [Ciervo *et al.*, 1985]. Obviously, when few data are available to locate an event (e.g., for most events near the detection threshold), each datum is very important. It is likely that the probability-weighted approach underestimates location uncertainties for small events because data with low probability of detection provide unique information that is important to constraining location. It appears that the probability-weighted approach does not adequately reduce the contribution of these data to the location uncertainty.



**Figure 4.9.** Contours of the semi-major axis (SMA, in kilometers) computed using the probability-weighted approach for events at the 3 *P* detection threshold. Uncertainties are given at the 90% confidence level. Depth is constrained to the surface.

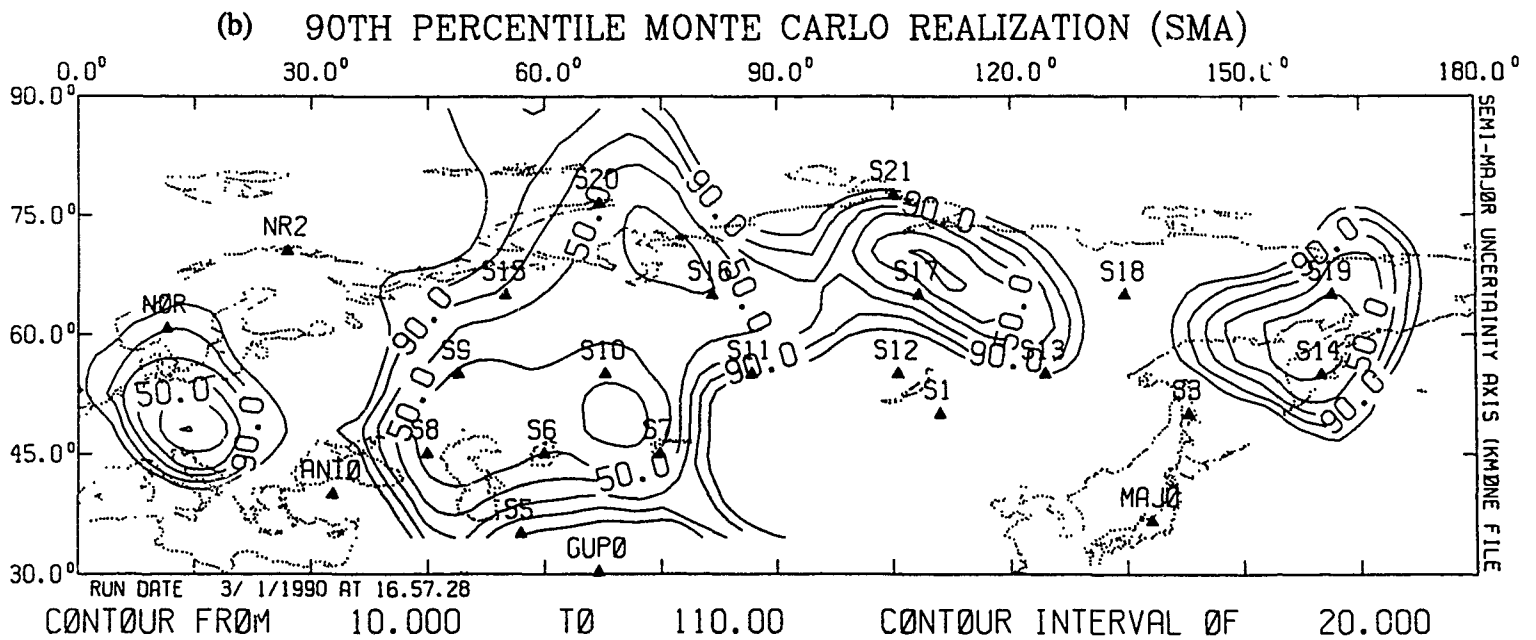
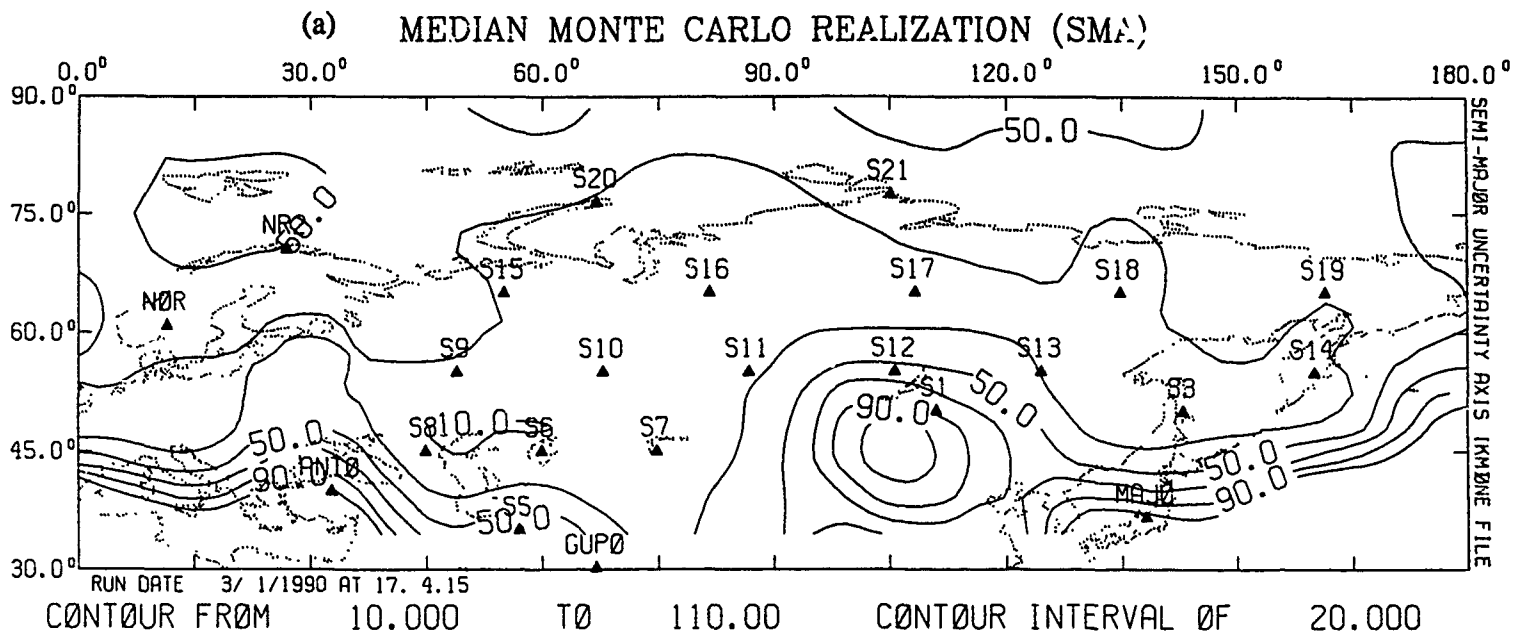


**Figure 4.10.** Contours of the SMA computed using the Monte Carlo approach for events at the 3 P detection threshold. (a) Median realization and (b) 90th percentile realization. Uncertainties are given at the 90% confidence level. Depth is constrained to the surface.

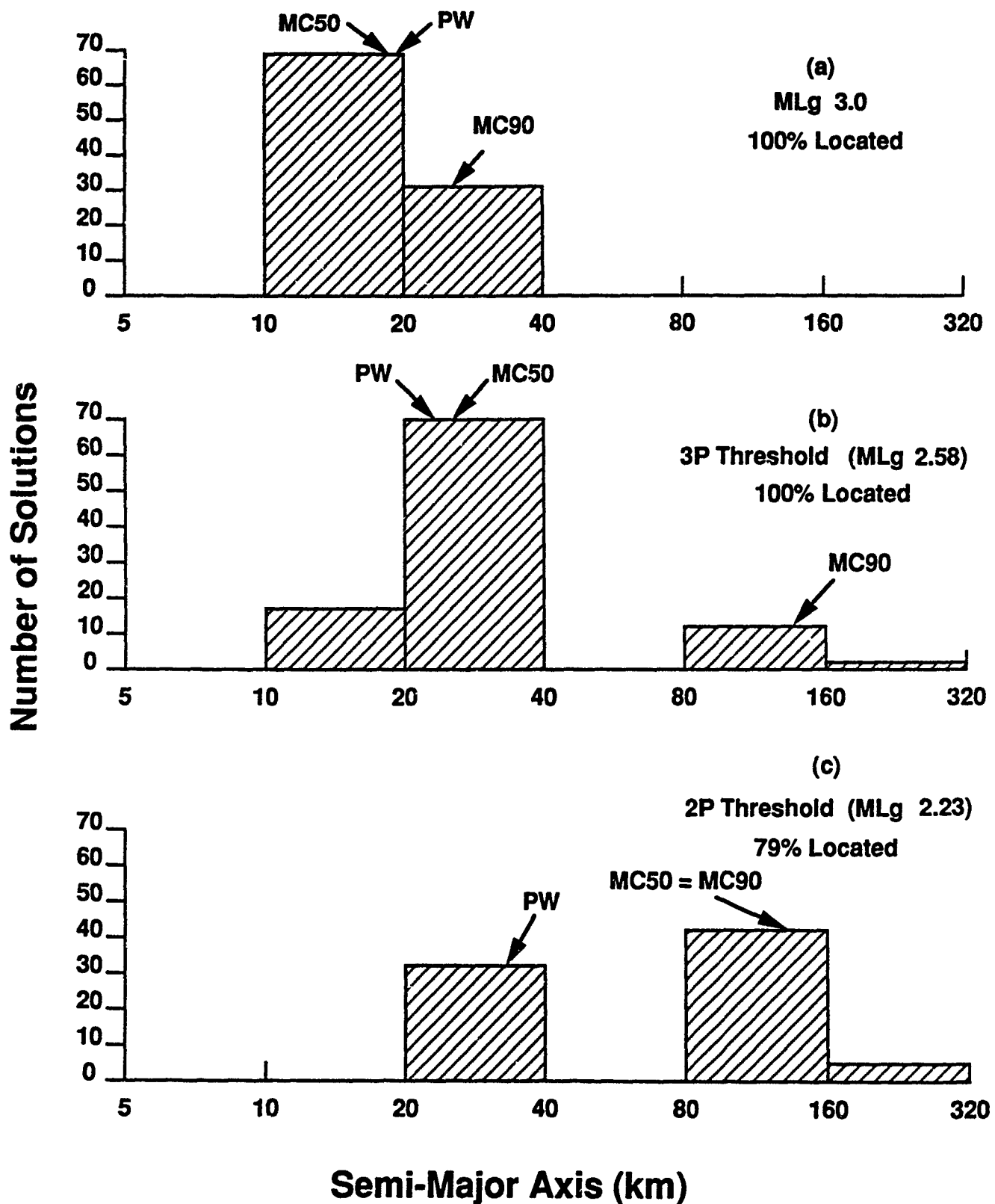


**Figure 4.11.** Histogram of location uncertainties (SMA) determined from 100 Monte Carlo realizations of location solutions in the western Soviet Union ( $60^\circ$  N,  $60^\circ$  E). The probability-weighted (PW), the median Monte Carlo realization (MC50), and the 90th percentile Monte Carlo realization (MC90) SMA values are marked. The fraction of Monte Carlo realizations with enough data to constrain the epicenter is also listed. Event magnitudes are (a) *MLg* 3.0, (b) *MLg* 2.58 (3 *P* detection threshold), and (c) *MLg* 2.23 (2 *P* detection threshold).

## 5. SUMMARY

This report describes a computer program called *NetSim* that simulates the detection and location capability of seismic networks that include regional stations and arrays. The main advantage of *NetSim* over other simulation programs is the incorporation of frequency dependence in the estimates for the source, attenuation, station noise, and array gain. This is very important for regional networks, as is demonstrated by the comparison of frequency-dependent and frequency-independent detection thresholds for a network of 33 stations in and around the Soviet Union. The results are shown in Table 5.1.

Table 5.1 The 90% *MLg* thresholds for a network of 33 stations.

center expand tab (:); c c c c. \_ Figure:Detection: :90% *MLg*  
Number:Criterion:Frequency:Threshold \_

4.5a:3 P:1 Hz (fixed):3.7-4.2 4.5b:3 P:10 Hz (fixed):2.8-5.3 4.6:3 P:1-20 Hz (vary-  
ing):2.6-3.4

These simulations are based on regional wave attenuation and noise conditions at NORESS, where the frequency of the maximum SNR decreases with increasing epicentral distance. The frequency-dependent detection thresholds are lower than the thresholds at either 1 Hz or 10 Hz because the frequency of the maximum SNR at ranges that control the detection threshold is typically between 3 and 7 Hz. It is clear from this example that the detection capability of regional networks cannot be simulated accurately unless frequency-dependent factors are included.

Other important advantages of *NetSim* over similar computer programs are: (1) noise levels for secondary phases are based on the coda of previous arrivals (and depend on event magnitude and epicentral distance), (2) arrival time and azimuth standard deviations are used to estimate location uncertainties, and (3) the effect of undetected phases on location uncertainties can be estimated using a Monte Carlo approach that mimics the way location uncertainties vary in practice. The probability-weighted approach (used in *SNAP/D*) assumes that all data contribute to the location, but the standard deviations are divided by the square root of the probability of detection. Thus, arrival times and azimuths from phases with low probability of detection will not contribute much to the location solution since their effective standard deviations are large. However, comparison to results from a more realistic Monte Carlo approach suggests that the probability-weighted uncertainties underestimate the true location uncertainties for small events. This implies that the probability-weighted approach does not adequately degrade the contribution of data with low probability of detection.

(THIS PAGE INTENTIONALLY LEFT BLANK)

## ACKNOWLEDGMENTS

We thank Thomas Bache for his careful review of this report, and Henry Swanger and Jeff Given for many helpful suggestions. We are also grateful to Donna Williams who did much of the *NetSim* testing. This research was funded by the Defense Advanced Research Projects Agency under Contract F08606-88-C-0033 and monitored by Air Force Technical Applications Center.

(THIS PAGE INTENTIONALLY LEFT BLANK)

## REFERENCES

- Aki, K., and P. Richards, *Quantitative Seismology: Theory and Methods*, W. H. Freeman, San Francisco, Calif., 1980.
- Bratt, S. and T. Bache, Locating events with a sparse network of regional arrays, *Bull. Seismol. Soc. Am.*, 78, 780-798, 1988.
- Bratt, S., T. Bache, and D. Williams, Seismic monitoring capability in the Soviet Union using hypothetical regional networks, *Final Tech. Rep. SAIC 87/1752*, Sci. Appl. Int. Corp., San Diego, Calif, AFGL-TR-87-0244, 1987a.
- Bratt, S., P. Ware, and D. Williams, Seismic network assessment program contouring *SNAPCON* user's and programmer's guide, *Tech. Rep. SAIC 87/1117*, Sci. Appl. Int. Corp., San Diego, Calif, 1987b.
- Bratt, S., P. Ware, and D. Williams, Probability and importance plotting *PRIMP* user's and programmer's guide, *Tech. Rep. SAIC 87/1116*, Sci. Appl. Int. Corp., San Diego, Calif, 1987c.
- Ciervo, A., S. Sanemitsu, D. Snead, R. Suey, and A. Watson, User's manual for *SNAP/D*: seismic network assessment program for detection, *Pacific-Sierra Research Corporation, Report 1027B*, 1985.
- Jordan, T., and K. Sverdrup, Teleseismic location techniques and their application to earthquake clusters in the south-central Pacific, *Bull. Seismol. Soc. Am.*, 71, 1105-1130, 1981.
- Kvaerna, T., On exploitation of small-aperture NORESS type arrays for enhanced *P*-wave detectability, *Bull. Seismol. Soc. Am.*, 79, 888-900, 1989.
- Sereno, T., Numerical modeling of *Pn* geometric spreading and empirically determined attenuation of *Pn* and *Lg* phases recorded in eastern Kazakhstan, *Semiannu. Tech. Rep. SAIC 89/1555*, Sci. Appl. Int. Corp., San Diego, Calif, 1989.
- Sereno, T., S. Bratt, and T. Bache, Simultaneous inversion of regional wave spectra for attenuation and seismic moment in Scandinavia, *J. Geophys. Res.*, 93, 2019-2035, 1988.
- Suteau-Henson, A., and T. Bache, Spectral characteristics of regional phases recorded at NORESS, *Bull. Seismol. Soc. Am.*, 78, 708-725, 1988.

Wirth, M., Estimation of network detection and location capability, Air Force Applications Center, Washington DC, [revision of August 1970 report], 1977.

## APPENDIX A: INPUT/OUTPUT DATA

This appendix describes the *NetSim* input and output data and file formats. The input to *NetSim* is read from standard ASCII files. These input files can be updated interactively, and new files can be written using the *NetSim* data handling module. *NetSim* output is also written to standard ASCII files. One of these output files is read by *SnapCon*, which plots the results (detection thresholds, probabilities for fixed event size, or location uncertainties) as contours on regional or world maps.

There are five categories of input data: control, source, propagation, site/station, and noise (see Section 3). Each category has one or more types of input data files. We identify these different data files by a three-letter suffix appended to the data file name (these suffixes are included in tables in this appendix for each input data file). The *NetSim* computer program does not impose this file naming convention, but we have found it to be convenient. Tables A.1–A.15 list the format of the input and output data files. Indented lines indicate a continuation from the previous line. Sample files are given in Section 4.

*NetSim* includes provisions for up to ten seismic waves (or phases). The wave input is ordered such that:

<i>Wave(1)</i>	=	<i>P (or Pn)</i>
<i>Wave(2)</i>	=	<i>pP</i>
<i>Wave(3)</i>	=	<i>Pg</i>
<i>Wave(4)</i>	=	<i>S (or Sn)</i>
<i>Wave(5)</i>	=	<i>Lg</i>
<i>Wave(6)</i>	=	<i>LR</i>
<i>Wave(7)</i>	=	<i>O1</i>
<i>Wave(8)</i>	=	<i>O2</i>
<i>Wave(9)</i>	=	<i>O3</i>
<i>Wave(10)</i>	=	<i>O4</i>

where the last four are slots for additional seismic phases.

### INPUT DATA

**Control Data.** The control data define the nature of the *NetSim* run (detection or location or both, network detection probability, detection criteria, etc). There is only one input file in this category; the control file. Table A.1 shows the format of the control file. The following list defines each input parameter.

Table A.1. Control File

<b>CONTROL FILE</b>	
<i>Suffix: .cnt</i>	
<i>title</i>	
<i>outpre</i>	
<i>outdir</i>	
<i>dir</i>	
<i>runtype</i>	
<i>subtype</i>	
<i>detcrit</i>	
<i>locwavs</i>	
<i>sizetype</i>	
<i>evsize evmin evmax probdet cutlo regdist</i>	
<i>probloc numcarlo prctlo prcthi</i>	
<i>depthfix eventdepth</i>	
<i>numrunfrq</i>	
<i>runfrq(1) ... runfrq(numrunfrq)</i>	
<i>file.epi</i>	
<i>file.smd</i>	
<i>file.sgr</i>	
<i>file.pmd</i>	
<i>file.pgr</i>	
<i>file.sta</i>	

### Control File (.cnt)

1. *title* – Title of the *NetSim* run.
2. *outpre* – Prefix for *NetSim* output files. The output files are named *outpre.gra* and *outpre.lst* (these are described below).
3. *outdir* – Directory for *NetSim* output files.
4. *dir* – Directory for the *NetSim* input files.
5. *runtype* – *NetSim* run type. Acceptable values are "detection," "location," or "detloc" (detection and location).
6. *subtyp* – *NetSim* run subtype. Acceptable values are "threshold" and "probability."
7. *detcrit* – Detection criteria. The format is the same as that described in the *SNAP/D* user's manual (*Ciervo et al.*, 1985). Two examples are:
  - a.  $P/3$ ; *P*-wave detection by at least three stations.
  - b.  $(P/3 + (P/2 * Lg/1) + (P/1 * Lg/2) + Lg/3)$ ; at least three *P* or *Lg* waves detected by the network. Literal translation: *P*-wave detection at three stations, or *P*-wave detection at two stations and *Lg*-wave detection at one station, or *P*-wave detection at one station and *Lg*-wave detection at two stations, or *Lg*-wave detection at three stations.
8. *locwavs* – Waves to use in location simulation (these may be different from the waves used for detection).
9. *sizetype* – Event size type. Acceptable values are "moment," "yield," " $m_b$ ," " $M_s$ ," or " $m_{Lg}$ ." If "moment" is specified, then *evsize*, *evmin*, and *evmax* are specified as log moment (nt-m). If "yield" is specified, then *evsize*, *evmin*, and *evmax* are specified as log yield (kilotons).
10. *evsize* – Event size to use in a probability run or in a location run with fixed event size. The units of *evsize* are determined by *sizetype*.
11. *evmin* and *evmax* – Minimum and maximum event size to use in a detection threshold run. The units are determined by *sizetype*.
12. *probdet* – Probability of detection for the network.
13. *cutlo* – Low-probability cut off. If detection probability is less than *cutlo* for any wave at any station, then this probability is set to zero.
14. *regdist* – Division between regional and teleseismic distances (in degrees).
15. *probloc* – Confidence level for location uncertainty.
16. *numcarlo* – Number of Monte Carlo location iterations (=1 for probability-weighted location uncertainties).
17. *prctlo* – Percentage of Monte Carlo location runs with uncertainty less than the lowest of the two uncertainties reported in the output file (e.g., the median Monte Carlo realization has *prctlo* = 0.50).
18. *prcthi* – Percentage of Monte Carlo location runs with uncertainty less than the largest of the two uncertainties reported in the output file (e.g., the 90th percentile

Monte Carlo realization has  $prcthi = 0.90$ ).

19. *depthfix* – Event depth constraint for location uncertainties. Acceptable values are "fixed" and "free."
20. *eventdepth* – Event depth in kilometers.
21. *numrunfreq* – Number of frequencies to use in the simulation.
22. *runfrq(i)*,  $i = 1, numrunfreq$  – Frequencies to use in the simulation (Hz).
23. *file.epi* – File name for epicenter input.
24. *file.smd* – File name for source media input.
25. *file.sgr* – File name for source grid input.
26. *file.pmd* – File name for path media input.
27. *file.pgr* – File name for path grid input.
28. *file.sta* – File name for station data input.

**Source Data.** The source data define source spectral amplitude and scaling relations as a function of source medium (e.g., granite, salt, tuff). There are four input file types in this category: epicenter grid file, source medium file, source medium grid file, and the source spectra files. The first three of these are indexed in the control file. The source spectra files are indexed in the source medium file. There is a separate source spectra file for each source medium. Tables A.2–A.5 show the format of the four source input files. The following list defines each input parameter.

#### Epicenter Grid File (.epi)

1. *title* – Title of the epicenter grid file.
2. *numepilat numepilon* – Number of latitudes and number of longitudes in the epicenter grid.
3. *epilat1 epilon1* – Initial latitude and initial longitude.
4. *epilatdel epilon1del* – Latitude increment and longitude increment.

#### Source Medium File (.smd)

1. *title* – Title of the source medium file.
2. *dir* – Directory for source spectra files (.sor).
3. *numsormed* – Number of different source media.
4. *sormed(i)*,  $i = 1, numsormed$  – Source media names (e.g., granite, tuff, salt).
5. *tbl.sor(i)*,  $i = 1, numsormed$  – File name of the source spectra file.
6. *smdrho(i)*,  $i = 1, numsormed$  – Density of the source medium ( $\text{kg/m}^3$ ).
7. *ayield(i)* and *byield(i)*,  $i = 1, numsormed$  – Slope and intercept of log moment versus log yield:  $\log \text{moment} = ayield \times \log \text{yield} + byield$ . Moment is in nt-m and yield is in kilotons.

**Table A.2. Epicenter File**

<b>EPICENTER FILE</b> <i>Suffix: .epi</i>
<i>title</i> <i>numepilat numepilon</i> <i>epilat1 epilon1</i> <i>epilatdel epilondel</i>

Table A.3. Source Media File

<b>SOURCE MEDIA FILE</b> <i>Suffix: .smd</i>
<i>title</i>
<i>dir</i>
<i>numsormed</i>
<i>sormed(1)</i>
<i>tbl.sor(1)</i>
<i>smdrho(1)</i>
<i>ayield(1) byield(1) amb(1) bmb(1)</i>
<i>ams(1) bms(1) amlg(1) bmlg(1)</i>
<i>sorwavfac(1,1) ... sorwavfac(10,1)</i>
<i>smdvel(1,1) ... smdvel(10,1)</i>
:
:
<i>sormed(numsormed)</i>
<i>tbl.sor(numsormed)</i>
<i>smdrho(numsormed)</i>
<i>ayield(numsormed) byield(numsormed) amb(numsormed) bmb(numsormed)</i>
<i>ams(numsormed) bms(numsormed) amlg(numsormed) bmlg(numsormed)</i>
<i>sorwavfac(1,numsormed) ... sorwavfac(10,numsormed)</i>
<i>smdvel(1,numsormed) ... smdvel(10,numsormed)</i>

Table A.4. Source Grid File

SOURCE GRID FILE	
<i>Suffix: .sgr</i>	
<i>title</i>	
<i>numsglat numsgrlon</i>	
<i>sgrlat1 sgrlon1</i>	
<i>sgrlatdel sgrlondel</i>	
<i>sormedname(1) sgrlat(1) sgrlon(1)</i>	
<i>:</i>	
<i>:</i>	
<i>sormedname(numsglat × numsgrlon) sgrlat(numsglat) sgrlon(numsgrlon)</i>	

Table A.5. Source Spectra File

SOURCE SPECTRA FILE <i>Suffix: .sor</i>
<i>title</i> <i>numsorfrq</i> <i>sorfrq(1) ... sorfrq(numsorfrq)</i> <i>numsormom</i> <i>sormom(1) ... sormom(numsormom)</i> Source amplitudes for frequency = <i>sorfrq(1)</i> ← comment line <i>soramp(1,1) ... soramp(numsormom,1)</i> : : Source amplitudes for frequency = <i>sorfrq(numsorfrq)</i> ← comment line <i>soramp(1,numsorfrq) ... soramp(numsormom,numsorfrq)</i>

8. *amb(i)* and *bmb(i)*,  $i = 1, \text{numsorted}$  – Slope and intercept of log moment versus  $m_b$ :  $\log \text{moment} = amb \times m_b + bmb$ . Moment is in nt-m.
9. *ams(i)* and *bms(i)*,  $i = 1, \text{numsorted}$  – Slope and intercept of log moment versus  $M_s$ :  $\log \text{moment} = ams \times M_s + bms$ . Moment is in nt-m.
10. *amlg(i)* and *bmlg(i)*,  $i = 1, \text{numsorted}$  – Slope and intercept of log moment versus  $m_{lg}$ :  $\log \text{moment} = amlg \times m_{lg} + bmlg$ . Moment is in nt-m.
11. *sorwavfac(j,i)*,  $j = 1, 10$  and  $i = 1, \text{numsorted}$  – Source excitation factor ( $\kappa_k$  in Section 2.1).
12. *smdvel(j,i)*,  $j = 1, 10$  and  $i = 1, \text{numsorted}$  – Source maximum velocity (m/s).

#### Source Grid File (.sgr)

1. *title* – Title of the source grid file.
2. *numsgrlat numsgrlon* – Number of latitudes and number of longitudes in the source medium grid.
3. *sgrlat1 sgrlon1* – Southernmost latitude and westernmost longitude in the source medium grid.
4. *sgrlatdel sgrlon1del* – Latitude increment and longitude increment for the source medium grid.
5. *sormedname(l)*,  $l = 1, \text{numsgrlat} \times \text{numsgrlon}$  – Source medium name (e.g., granite, tuff, salt) for each grid element.
6. *sgrlat(i)* and *sgrlon(j)*,  $i = 1, \text{numsgrlat}$  and  $j = 1, \text{numsgrlon}$  – Latitude and longitude of the southwest corner of each grid element.

#### Source Spectra File (.sor)

1. *title* – Title of the source spectra file.
2. *numsofreq* – Number of frequencies.
3. *sorfrq(i)*,  $i = 1, \text{numsofreq}$  – Frequencies (Hz).
4. *numsofmom* – Number of scalar seismic moments.
5. *sormom(j)*,  $j = 1, \text{numsofmom}$  – Log seismic moment (nt-m).
6. *sorampl(j,i)*,  $j = 1, \text{numsofmom}$  and  $i = 1, \text{numsofreq}$  – Log source spectral amplitude (nt-m).

**Propagation Data.** The propagation data define the attenuation and travel time as a function of path medium (e.g., stable or tectonic). There are four input file types in this category: path medium file, path medium grid file, attenuation files, and travel time files. The first two of these are indexed in the control file. The attenuation and travel time files are indexed in the path medium file. There are separate attenuation and travel time files for each path medium. Tables A.6–A.9 show the format of the four propagation input files. The following list defines each input parameter.

Table A.6. Path Media File

PATH MEDIA FILE
<i>Suffix: .pmd</i>
<i>title</i>
<i>dir</i>
<i>tlen(1) gvell(1) gvel2(1)</i>
⋮
<i>tlen(10) gvell(10) gvel2(10)</i>
<i>numpthmed</i>
<i>pthmed(j)</i> ,
<i>tbl.atn(1,1) tbl.tim(1,1)</i>
<i>atnstd(1,1) sorcor(1,1) reccor(1,1)</i>
<i>timsd(1,1) azsd(1,1)</i>
⋮
<i>tbl.atn(10,1) tbl.tim(10,1)</i>
<i>atnstd(10,1) sorcor(10,1) reccor(10,1)</i>
<i>timsd(10,1) azsd(10,1)</i>
⋮
<i>pthmed(numpthmed)</i>
<i>tbl.atn(1,numpthmed) tbl.tim(1,numpthmed)</i>
<i>atnstd(1,numpthmed) sorcor(1,numpthmed) reccor(1,numpthmed)</i>
<i>timsd(1,numpthmed) azsd(1,numpthmed)</i>
⋮
<i>tbl.atn(10,numpthmed) tbl.tim(10,numpthmed)</i>
<i>atnstd(10,numpthmed) sorcor(10,numpthmed) reccor(10,numpthmed)</i>
<i>timsd(10,numpthmed) azsd(10,numpthmed)</i>

Table A.7. Path Grid File

<b>PATH GRID FILE</b> <i>Suffix: .pgr</i>
<i>title</i>
<i>numpgrlat numpgrlon</i>
<i>pgrlat1 pgrlon1</i>
<i>pgrlatd:l pgrlondel</i>
<i>pthmedname(1) pgrlat(1) pgrlon(1)</i>
<i>:</i>
<i>:</i>
<i>pthmedname(numpgrlat × numpgrlon) pgrlat(numpgrlat) pgrlon(numpgrlon)</i>

Table A.8. Attenuation File

ATTENUATION FILE <i>Suffix: .atn</i>
<i>title</i> <i>numatnfrq</i> <i>atnfrq(1) ... atnfrq(numatnfrq)</i> <i>numatndst</i> <i>atndst(1) ... atndst(numatndst)</i> attenuation for frequency = <i>atnfrq(1)</i> ← comment line <i>atnamp(1,1) ... atnamp(numatndst,1)</i> : : attenuation for frequency = <i>atnfrq(numatnfrq)</i> ← comment line <i>atnamp(1,numatnfrq) ... atnamp(numatndst,numatnfrq)</i>

Table A.9. Travel Time File

TRAVEL TIME FILE
<i>Suffix: .tim</i>
<i>title</i>
<i>numtimdph</i>
<i>timdph(1) ... timdph(numtimdph)</i>
<i>numtir:dst</i>
<i>timdst(1) ... timdst(numtimdst)</i>
travel-time for depth = <i>depth(1)</i> $\Leftarrow$ comment line
<i>tratim(1,1) ... tratim(numtimdst,1)</i>
<i>:</i>
<i>:</i>
travel-time for depth = <i>depth(numtimdph)</i> $\Leftarrow$ comment line
<i>tratim(1,numtimdph) ... tratim(numtimdst,numtimdph)</i>

### Path Medium File (.pmd)

1. *title* – Title of the path medium file.
2. *dir* – Directory for the attenuation and travel time files.
3. *tlen(j)*,  $j = 1, 10$  – Time window length used for the spectral estimate for each wave.
4. *gvell(j)* and *gvel2(j)*,  $j = 1, 10$  – Range of group velocities used for the spectral estimate for each wave (if *tlen(j)* is less than zero).
5. *numpthmed* – Number of different path media.
6. *pthmed(i)*,  $i = 1, \text{numpthmed}$  – Path media names (e.g., stable and tectonic).
7. *tbl.atn(i)*,  $i = 1, \text{numpthmed}$  – File names for attenuation data tables.
8. *tbl.tim(i)*,  $i = 1, \text{numpthmed}$  – File names for travel time data tables.
9. *atnstd(j,i)*,  $j = 1, 10$  and  $i = 1, \text{numpthmed}$  – Standard deviation of log attenuation.
10. *sorcor(j,i)*,  $j = 1, 10$  and  $i = 1, \text{numpthmed}$  – Log source correction factor for teleseismic distances.
11. *reccor(j,i)*,  $j = 1, 10$  and  $i = 1, \text{numpthmed}$  – Log receiver correction factor for teleseismic distances.
12. *timsd(j,i)*,  $j = 1, 10$  and  $i = 1, \text{numpthmed}$  – Travel time standard deviation (s).
13. *azsd(j,i)*,  $j = 1, 10$  and  $i = 1, \text{numpthmed}$  – Azimuth standard deviation (degrees).

### Path Grid File (.pgr)

1. *title* – Title of the path grid file.
2. *numpgrlat numpgrlon* – Number of latitudes and longitudes in the path medium grid.
3. *pgrlat1 pgrlon1* – Southernmost latitude and westernmost longitude in the path medium grid.
4. *pgrlatdel pgrlondel* – Latitude increment and longitude increment for the path medium grid.
5. *pthmedname(l)*,  $l = 1, \text{numpgrlat} \times \text{numpgrlon}$  – Path medium name (e.g., stable or tectonic) for each grid element.
6. *pgrlat(i)* and *pgrlon(j)*,  $i = 1, \text{numpgrlat}$  and  $j = 1, \text{numpgrlon}$  – Latitude and longitude of the southwest corner of each grid element.

### Attenuation File (.atn)

1. *title* – Title of the attenuation file.
2. *numatnfrq* – Number of frequencies in the attenuation file.
3. *atnfrq(i)*,  $i = 1, \text{numatnfrq}$  – Frequencies (Hz).

4. *numatndst* – Number of distances in the attenuation file.
5. *atndst(j)*,  $j = 1, \text{numatndst}$  – Distances (degrees).
6. *atnamp(j,i)*,  $j = 1, \text{numatndst}$  and  $i = 1, \text{numatnfrq}$  – Attenuation amplitude ( $\log m^{-1}$ ).

#### Travel Time File (.tim)

1. *title* – Title of the travel time file.
2. *numtimdph* – Number of depths in the travel time file.
3. *timdph(i)*,  $i = 1, \text{numtimdph}$  – Depths (km).
4. *numtimdst* – Number of distances in the travel time file.
5. *timdst(j)*,  $j = 1, \text{numtimdst}$  – Distances (degrees).
6. *tratim(j,i)*,  $j = 1, \text{numtimdst}$  and  $i = 1, \text{numtimdph}$  – Travel times (s).

**Site/Station Data.** The site/station data define the station parameters (e.g., station locations, station corrections, station reliability, signal-to-noise ratios required for detection, etc.) and the local site response and array gain functions. There are two input file types in this category: the station file and the site response file. The station file is indexed in the control file. The site response file (for each station and wave) is indexed in the station file. The station file also indexes the ambient noise and noise factor files (next section). Tables A.10–A.11 show the format of the site/station input files. The following list defines each input parameter.

#### Station File (.sta)

1. *title* – Title of the station file.
2. *dir* – Directory for the site response, noise, and noise factor files.
3. *tbl.nfc(i)*,  $i = 1, 10$  – File name for the noise factor ( coda decay rate) file.
4. *prewav(i)*,  $i = 1, 10$  – Phase identification of the previous arrival (e.g.,  $i = 5$  for  $Lg$  and *prewav(5)* =  $S_n$ ).
5. *numsta* – Number of stations in the network.
6. *staid(j)*,  $j = 1, \text{numsta}$  – Station identification (e.g., ANTO).
7. *tbl.noi(j)*,  $j = 1, \text{numsta}$  – File name for the ambient noise power spectral density.
8. *noisd(j)*,  $j = 1, \text{numsta}$  – Standard deviation of the log ambient noise amplitude.
9. *stalat(j)* *stalon(j)*,  $j = 1, \text{numsta}$  – Station latitude and longitude.
10. *starel(j)*,  $j = 1, \text{numsta}$  – Station reliability ( $\leq 1.0$ ).
11. *starho(j)*,  $j = 1, \text{numsta}$  – Density of the receiver medium ( $\text{kg/m}^3$ ).
12. *stacor(i,j)*,  $i = 1, 10$  and  $j = 1, \text{numsta}$  – Station correction to log amplitude.
13. *stsigsd(i,j)*,  $i = 1, 10$  and  $j = 1, \text{numsta}$  – Station-specific standard deviation of the log signal amplitude.

Table A.10. Station File

STATION FILE Suffix: .sta
<i>title</i>
<i>dir</i>
<i>tbl.nfc(1) prewav(1)</i>
:
:
<i>tbl.nfc(10) prewav(10)</i>
<i>numsta</i>
<i>staid(1) tbl.noi(1) noisd(1)</i>
<i>stalat(1) stalon(1) starel(1)</i>
<i>starho(1)</i>
<i>stacor(1,1) stsigsd(1,1) snrth(1,1)</i>
<i>statimsd(1,1) staaazsd(1,1) stavel(1,1) tbl.srs(1,1)</i>
:
:
<i>stacor(10,1) stsigsd(10,1) snrth(10,1)</i>
<i>statimsd(10,1) staaazsd(10,1) stavel(10,1) tbl.srs(10,1)</i>
:
:
<i>staid(numsta) tbl.noi(numsta) noisd(numsta)</i>
<i>stalat(numsta) stalon(numsta) starel(numsta)</i>
<i>starho(numsta)</i>
<i>stacor(1,numsta) stsigsd(1,numsta) snrth(1,numsta)</i>
<i>statimsd(1,numsta) staaazsd(1,numsta) stavel(1,numsta) tbl.srs(1,numsta)</i>
:
:
<i>stacor(10,numsta) stsigsd(10,numsta) snrth(10,numsta)</i>
<i>statimsd(10,numsta) staaazsd(10,numsta) stavel(10,numsta) tbl.srs(10,numsta)</i>

Table A.11. Site Response File

<b>SITE RESPONSE FILE</b> <i>Suffix: .srs</i>
<i>title</i> <i>numsrs</i> <i>srsfrq(1) srsamp(1)</i> : : <i>srsfrq(numsrs) srsamp(numsrs)</i>

14. *snrth(i,j)*,  $i = 1, 10$  and  $j = 1, numsta$  – Signal-to-noise ratio threshold for detection.
15. *statimsd(i,j)*,  $i = 1, 10$  and  $j = 1, numsta$  – Station-specific travel time standard deviation (s).
16. *staaazsd(i,j)*,  $i = 1, 10$  and  $j = 1, numsta$  – Station-specific azimuth standard deviation (degrees)
17. *stave!(i,j)*,  $i = 1, 10$  and  $j = 1, numsta$  – Velocity of the receiver medium (in m/s).
18. *tbl.srs(i,j)*,  $i = 1, 10$  and  $j = 1, numsta$  – File name for the site response data file.

#### Site Response File (.srs)

1. *title* – Title of the site response file.
2. *numsrs* – Number of frequencies in the site response file.
3. *srsfrq(i)*,  $i = 1, numsrs$  – Frequency (Hz).
4. *srsamp(i)*,  $i = 1, numsrs$  – Log amplitude of the site response.

**Noise Data.** The noise data define the ambient station noise spectra and coda decay rates that determine the noise levels for secondary phases (see Section 2). There are two input file types in this category: the noise file and the noise factor file (coda decay rate). Both of these files are indexed in the station file. There is a separate ambient noise file for each station, and a separate noise factor file for each wave type. Tables A.12–A.13 show the format of the noise input files. The following list defines each input parameter.

#### Ambient Noise File (.noi)

1. *title* – Title of the ambient noise file.
2. *numnoi* – Number of frequencies in the ambient noise file.
3. *noifrq(i)*,  $i = 1, numnoi$  – Frequency (Hz)
4. *noiamp(i)*,  $i = 1, numnoi$  – Log noise power spectral density ( $\text{nm}^2/\text{Hz}$ .)

#### Noise Factor File for Secondary Phases (.nfc)

1. *title* – Title of the noise factor file.
2. *numnfc* – Number of distances in the noise factor file.
3. *nfcdst(i)*,  $i = 1, numnfc$  – Distance (degrees)
4. *nfcfac(i)*,  $i = 1, numnfc$  – Noise factor (or coda decay rate).

**Table A.12. Ambient Noise File**

<b>AMBIENT NOISE FILE</b> <i>Suffix: .noi</i>
<i>title</i> <i>numnoi</i> <i>noifrq(1) noiamp(1)</i> : : <i>noifrq(numnoi) noiamp(numnoi)</i>

Table A.13. Noise Factor File

NOISE FACTOR FILE	
<i>Suffix: .nfc</i>	
<i>title</i>	
<i>numnfc</i>	
<i>nfcdst(1) nfcfac(1)</i>	
<i>:</i>	
<i>:</i>	
<i>nfcdst(numnfc) nfcfac(numnfc)</i>	

## OUTPUT DATA

There are two *NetSim* output files: a graphics file (suffix = ".gra") and a list file (suffix = ".lst"). These suffixes are appended to the output prefix specified in the control file. The graphics file is an ASCII file that is read by *SnapCon* to create contour maps of the *NetSim* output (see Section 3). The list file is also an ASCII file and it includes individual station probabilities, the frequency of the maximum signal-to-noise ratio, and location importances for each wave, station and epicenter.

**Graphics File.** The graphics output file contains information from the control file to identify the run parameters. More importantly, it contains epicenters, detection thresholds, probabilities, and location uncertainties that are used as input to *SnapCon* for plotting contour maps. Table A.14 shows the format of the graphics output file. Most of the parameters in the ".gra" file were described above (control input). Only parameters not described previously are identified in the following list.

### Graphics File (.gra)

1.  $episize(i)$ ,  $i = 1, numepi$  – Event size in units specified by *sizetype*. These are detection thresholds for a *NetSim* threshold run.
2.  $fnetprob(i)$ ,  $i = 1, numepi$  – Probability of detection for the network.
3.  $fracloc(i)$ ,  $i = 1, numepi$  – Fraction of Monte Carlo realizations with sufficient data to constrain location.
4.  $smaj1(i)$  and  $smaj2(i)$ ,  $i = 1, numepi$  – Length of the semi-major axis (km) for *prctlo* and *prcthi*, respectively ( $smaj1(i) = smaj2(i)$  for probability-weighted location uncertainties).
5.  $smin1(i)$  and  $smin2(i)$ ,  $i = 1, numepi$  – Length of the semi-minor axis (km) for *prctlo* and *prcthi*, respectively ( $smin1(i) = smin2(i)$  for probability-weighted location uncertainties).
6.  $strk1(i)$  and  $strk2(i)$ ,  $i = 1, numepi$  – Strike of the semi-minor axis for *prctlo* and *prcthi*, respectively ( $strk1(i) = strk2(i)$  for probability-weighted location uncertainties).
7.  $depth1(i)$  and  $depth2(i)$ ,  $i = 1, numepi$  – Depth uncertainty (km) for *prctlo* and *prcthi*, respectively ( $depth1(i) = depth2(i)$  for probability-weighted location uncertainties).

**List File.** The list output file contains detailed information about the detection and location parameters at each station and for each epicenter. Table A.15 shows the format of the list output file. The first page lists the control data for the run. The second page lists the wave-independent station data, and this is followed by one page of station data for each wave used in the *NetSim* run. After that, there are two pages for each epicenter. The first of these lists for each wave at the individual stations the probability of detection, the frequency of the maximum signal-to-noise ratio, and the amplitude standard deviation. The second page for each epicenter lists for each wave

Table A.14. Graphics File

GRAPHICS FILE	
Suffix: <i>.gra</i>	
Title of Run	: <i>title</i>
Date and Time of Run	: <i>idate, itime</i>
Control File Name	: <i>file.cnt</i>
Epicenter File Name	: <i>file.epi</i>
Source Media File Name	: <i>file.smd</i>
Source Grid File Name	: <i>file.sgr</i>
Path Media File Name	: <i>file.pmd</i>
Path Grid File Name	: <i>file.pgr</i>
Station File Name	: <i>file.sta</i>
Output Prefix	: <i>outpre</i>
Output Directory	: <i>outdir</i>
Input Directory	: <i>dir</i>
Run Type	: <i>runtype</i>
Sub-run Type	: <i>subtype</i>
Detection Criteria	: <i>detcrit</i>
Waves to Use in Location	: <i>locwaves</i>
Event Size Type	: <i>sizetype</i>
Event Size	: <i>evsize</i>
Minimum Event Size	: <i>evmin</i>
Maximum Event Size	: <i>evmax</i>
Probability of Detection	: <i>probdet</i>
Low Probability Cutoff	: <i>cullo</i>
Regional Distance	: <i>regdist</i>
Location Confidence Level	: <i>probloc</i>
Number of Monte Carlo Simulations	: <i>numcarlo</i>
Low % Monte Carlo	: <i>prcilo</i>
High % Monte Carlo	: <i>prcthi</i>
Fixed or Free Depth	: <i>depthfix</i>
eventdepth	: <i>eventdepth</i>
Number of Frequencies	: <i>numrunfrq</i>
Run Frequencies	: <i>runfrq(1)</i>
	:
	:
	<i>runfrq(numrunfrq)</i>
<i>numsta</i>	
<i>staid(1) stala(1) stalon(1)</i>	
:	
:	
<i>staid(numsta) stala(numsta) stalon(numsta)</i>	
<i>numepi</i>	
<i>epilat(1) epsilon(1) epysize(1) fnetprob(1) fracloc(1)</i>	
<i>smaj1(1) smin1(1) strk1(1) depth1(1)</i>	
<i>smaj2(1) smin2(1) strk2(1) depth2(1)</i>	
:	
:	
<i>epilat(numepi) epsilon(numepi) epysize(numepi) fnetprob(numepi) fracloc(numepi)</i>	
<i>smaj1(numepi) smin1(numepi) strk1(numepi) depth1(numepi)</i>	
<i>smaj2(numepi) smin2(numepi) strk2(numepi) depth2(numepi)</i>	

Table A.15. List File

LIST FILE (Page 1)	
Suffix: .lst	
Title of Run	: title
Date and Time of Run	: icate, itime
Control File Name	: file.cnt
Epicenter File Name	: file.epi
Source Media File Name	: file.smd
Source Grid File Name	: file.sgr
Path Media File Name	: file.pmd
Path Grid File Name	: file.pgr
Station File Name	: file.sta
Output Prefix	: outpre
Output Directory	: outdir
Input Directory	: dir
Run Type	: runtype
Sub-run Type	: subtype
Detection Criteria	: detcrit
Waves to Use in Location	: locwaves
Event Size Type	: sizetype
Event Size	: evsize
Minimum Event Size	: evmin
Maximum Event Size	: evmax
Probability of Detection	: probdet
Low Probability Cutoff	: cullo
Regional Distance	: regdist
Location Confidence Level	: probloc
Number of Monte Carlo Simulations	: numcarlo
Low % Monte Carlo	: prctl0
High % Monte Carlo	: prcthi
Fixed or Free Depth	: depthfix
eventdepth	: eventdepth
Number of Frequencies	: numrunfrq
Run Frequencies	: runfrq(1)
	:
	:
	: runfrq(numrunfrq)

LIST FILE (Page 2)							
Suffix: .lst							
STATION DATA							
STATION FILE DIRECTORY: stadir							
I	IDENT	LAT.	LONG.	RELIAB.	DENSITY	NOISE SD	AMBIENT-NOISE TABLE
ista	staid	stalat	stalon	starel	starho	oisd	tblnoi
:	:	:	:	:	:	:	:
:	:	:	:	:	:	:	:

LIST FILE (Pages 3-X)

Suffix: .lst

STATION TABLE (wavename -WAVE)

I	IDENT	STATION CORRECTION	S/N RATIO	WAVE VELOCITY	SIGNAL SD	TIME SD	AZIMUTH SD	SITE RESPONSE TABLE
ista	staid	stacor	snrth	stavel	stsigsd	statimsd	staazsd	tbl.srs
:	:	:	:	:	:	:	:	:
:	:	:	:	:	:	:	:	:

LIST FILE (Page X+1)

Suffix: .lst

EPICENTER *iepi* LAT=*epilat* LONG=*epilon*

EVENT SIZE	: <i>episize</i>	NETWORK PROBABILITY (%)	: <i>fnetprob</i>
NUM. OF ITERATIONS	: <i>numiter</i>	ITER. BOUNDS EXCEEDED	: <i>outbound</i>
SEMI-MAJOR AXIS (LO)	: <i>smajlo</i>	SEMI-MAJOR AXIS (HI)	: <i>smajhi</i>
SEMI-MINOR AXIS (LO)	: <i>sminlo</i>	SEMI-MINOR AXIS (HI)	: <i>sminhi</i>
STRIKE (LO)	: <i>strklo</i>	STRIKE (HI)	: <i>strkhi</i>
DEPTH-INTERVAL (LO)	: <i>depthlo</i>	DEPTH-INTERVAL (HI)	: <i>depthhi</i>
MONTE CARLO FRACTION	: <i>fracloc</i>		

STATION		ANG. DIST	AZM	STATION PROB.	wavename -WAVE FREQ. OF MAX. S/N	AMPL ATTEN.SD
<i>ista</i>	<i>staid</i>	<i>stadist</i>	<i>stazm</i>	<i>staprob</i>	<i>frqmax</i>	<i>ampsd</i>
:	:	:	:	:	:	:
:	:	:	:	:	:	:

LIST FILE (Page X+2)

Suffix: .lst

EPICENTER *iepi* LAT=*epilat* LONG=*epilon*

STATION		ANG. DIST	AZM	ATT'D	wavename -WAVE AZSD	EPICENTER IMPORT.	DEPTH IMPORT.
<i>ista</i>	<i>staid</i>	<i>stadist</i>	<i>stazm</i>	<i>timsd</i>	<i>azsd</i>	<i>epiimp</i>	<i>depthimp</i>
:	:	:	:	:	:	:	:
:	:	:	:	:	:	:	:

at each station the arrival time and azimuth standard deviations, and the epicenter and depth importances (see *Ciervo et al.*, 1985).

(THIS PAGE INTENTIONALLY LEFT BLANK)

**DISTRIBUTION LIST  
FOR UNCLASSIFIED REPORTS  
DARPA-FUNDED PROJECTS  
(Last Revised: 26 Sep 89)**

**RECIPIENT** **NUMBER OF COPIES**

**DEPARTMENT OF DEFENSE**

DARPA/NMRO 2  
ATTN: Dr. R. Alewine and Dr. R. Blandford  
1400 Wilson Boulevard  
Arlington, VA 22209-2308

Defense Intelligence Agency 1  
Directorate for Scientific and  
Technical Intelligence  
Washington, D.C. 20340-6158

Defense Nuclear Agency 1  
Shock Physics Directorate/SD  
Washington, D.C. 20305-1000

Defense Technical Information Center 2  
Cameron Station  
Alexandria, VA 22314

**DEPARTMENT OF THE AIR FORCE**

AFOSR/NP 1  
Bldg 410, Room C222  
Bolling AFB, Washington, D.C. 20332-6448

AFTAC/S/INFO 1  
Patrick AFB, FL 32925-6001

AFTAC/TT 3  
Patrick AFB, FL 32925-6001

AFWL/NTESG 1  
Kirkland AFB, NM 87171-6008

GL/LWH 1  
ATTN: Mr. J. Lewkowicz  
Terrestrial Sciences Division  
Hanscom AFB, MA 01731-5000

#### DEPARTMENT OF THE NAVY

NORDA 1  
ATTN Dr. J. A. Ballard  
Code 543  
NSTL Station, MS 39529

#### DEPARTMENT OF ENERGY

Department of Energy 1  
ATTN: Mr. Max A. Koontz (DP-331)  
International Security Affairs  
1000 Independence Avenue  
Washington, D.C. 20585

Lawrence Livermore National Laboratory 3  
ATTN: Dr. J. Hannon, Dr. S. Taylor, and Dr. K. Nakanishi  
University of California  
P.O. Box 808  
Livermore, CA 94550

Los Alamos Scientific Laboratory 2  
ATTN: Dr. C. Newton  
P.O. Box 1663  
Los Alamos, NM 87544

Sandia Laboratories 1  
ATTN: Mr. P. Stokes, Dept. 9110  
P.O. Box 5800  
Albuquerque, NM 87185

#### OTHER GOVERNMENT AGENCIES

Central Intelligence Agency 1  
ATTN: Dr. L. Turnbull  
OSI/NED, Room 5G48  
Washington, D.C. 20505

U.S. Arms Control and Disarmament Agency 1  
ATTN: Dr. M. Eimer  
Verification and Intelligence Bureau, Room 4953  
Washington, D.C. 20451

U.S. Arms Control and Disarmament Agency 1  
ATTN: Mr. R. J. Morrow  
Multilateral Affairs Bureau, Rm 5499  
Washington, D.C. 20451

U.S. Geological Survey 1  
ATTN: Dr. T. Hanks  
National Earthquake Research Center  
345 Middlefield Road  
Menlo Park, CA 94025

U.S. Geological Survey MS-913 1  
ATTN: Dr. R. Masse  
Global Seismology Branch  
Box 25046, Stop 967  
Denver Federal Center  
Denver, CO 80225

#### UNIVERSITIES

Boston College 1  
ATTN: Dr. A. Kafka  
Western Observatory  
381 Concord Road  
Weston, MA 02193

California Institute of Technology 1  
ATTN: Dr. D. Harkrider  
Seismological Laboratory  
Pasadena, CA 91125

Columbia University 1  
ATTN: Dr. L. Sykes  
Lamont-Doherty Geological Observatory  
Palisades, NY 10964

Cornell University 1  
ATTN: Dr. M. Barazangi  
INSTOC  
Snee Hall  
Ithaca, NY 14853

<p>Harvard University  ATTN: Dr. J. Woodhouse  Hoffman Laboratory  20 Oxford Street  Cambridge, MA 02138</p>	1
<p>Massachusetts Institute of Technology  ATTN: Dr. S. Soloman, Dr. N. Toksoz, and Dr. T. Jordon  Department of Earth and Planetary Sciences  Cambridge, MA 02139</p>	3
<p>Southern Methodist University  ATTN: Dr. E. Herrin and Dr. B. Stump  Geophysical Laboratory  Dallas, TX 75275</p>	2
<p>State University of New York at Binghamton  ATTN: Dr. F. Wu  Department of Geological Sciences  Vestal, NY 13901</p>	1
<p>St. Louis University  ATTN: Dr. B. Mitchell and Dr. R. Herrmann  Department of Earth and Atmospheric Sciences  3507 Laclede  St. Louis, MO 63156</p>	2
<p>The Pennsylvania State University  ATTN: Dr. S. Alexander  Geosciences Department  403 Deike Building  University Park, PA 16802</p>	1
<p>University of Arizona  ATTN: Dr. T. Wallace  Department of Geosciences  Tucson, AZ 85721</p>	1
<p>University of California, Berkeley  ATTN: Dr. T. McEvelly  Department of Geology and Geophysics  Berkeley, CA 94720</p>	1
<p>University of California, Los Angeles  ATTN: Dr. L. Knopoff  405 Hilgard Avenue  Los Angeles, CA 90024</p>	1

University of California, San Diego  
ATTN: Dr. J. Orcutt 1  
Scripps Institute of Oceanography  
La Jolla, CA 92093

University of Colorado 1  
ATTN: Dr. C. Archambeau  
CIRES  
Boulder, CO 80309

University of Illinois 1  
ATTN: Dr. S. Grand  
Department of Geology  
1301 West Green Street  
Urbana, IL 61801

University of Michigan 1  
ATTN: Dr. T. Lay  
Department of Geological Sciences  
Ann Arbor, MI 48109-1063

University of Nevada 1  
ATTN: Dr. K. Priestley  
Mackay School of Mines  
Reno, NV 89557

University of Southern California 1  
ATTN: Dr. K. Aki  
Center for Earth Sciences  
University Park  
Los Angeles, CA 90089-0741

#### DEPARTMENT OF DEFENSE CONTRACTORS

Analytical Sciences Corporation, The 1  
Dr. Richard Sailor  
ATTN: Document Control  
55 Walkers Brook Drive  
Reading, MA 01867

Applied Theory, Inc. 1  
ATTN: Dr. J. Trulio  
930 South La Brea Avenue  
Suite 2  
Los Angeles, CA 90036

Center for Seismic Studies ATTN: Dr. C. Romney and Mr. R. Perez 1300 N. 17th Street, Suite 1450 Arlington, VA 22209	2
ENSCO, Inc. ATTN: Mr. John R. Stevenson P.O. Box 1346 Springfield, VA 22151	1
ENSCO, Inc. ATTN: Dr. R. Kemerait 445 Pineda Court Melbourne, FL 32940-7508	1
Gould Inc. ATTN: Mr. R. J. Woodard Chesapeake Instrument Division 6711 Baymeado Drive Glen Burnie, MD 21061	1
Maxwell Laboratories, Inc. S-CUBED Reston Geophysics Office ATTN: Mr. J. Murphy, Suite 1112 11800 Sunrise Valley Drive Reston, VA 22091	1
Pacific Sierra Research Corp. ATTN: Mr. F. Thomas 12340 Santa Monica Boulevard Los Angeles, CA 90025	1
Rockwell International ATTN: B. Tittmann 1049 Camino Dos Rios Thousand Oaks, CA 91360	1
Rondout Associates, Inc. ATTN: Dr. P. Pomeroy P.O. Box 224 Stone Ridge, NY 12484	1
Science Applications International Corporation ATTN: Document Control (Dr. T. Bache, Jr.) 10260 Campus Point Drive San Diego, CA 92121	1

Science Horizons 2  
ATTN: Dr. T. Cherry and Dr. J. Minster  
710 Encinitas Blvd.  
Suite 101  
Encinitas, CA 92024

S-CUBED, A Division of Maxwell 1  
Laboratories, Inc.  
ATTN: Dr. Keith L. McLaughlin  
P.O. Box 1620  
La Jolla, CA 92038-1620

Sierra Geophysics, Inc. 2  
ATTN: Dr. R. Hart and Dr. G. Mellman  
11255 Kirkland Way  
Kirkland, WA 98033

SRI International 1  
ATTN: Dr. A. Florence  
333 Ravenswood Avenue  
Menlo Park, CA 94025

Teledyne Industries, Inc. 1  
Teledyne Geotech Alexandria Laboratories  
ATTN: Mr. W. Rivers  
314 Montgomery Street  
Alexandria, VA 22314-1581

Woodward-Clyde Consultants 1  
ATTN: Dr. L. Burdick  
P.O. Box 93254  
Pasadena, CA 91109-3254

#### NON-US RECIPIENTS

Blacknest Seismological Center 1  
ATTN: Mr. Peter Marshall  
Atomic Weapons Research Establishment  
UK Ministry of Defense  
Brimpton, Reading RG7-4RS  
United Kingdom

National Defense Research Institute 1  
ATTN: Dr. Ola Dahlman  
Stockholm 80, Sweden

NTNF NORSAR  
ATTN: Dr. Frode Ringdal  
P.O. Box 51  
N-2007 Kjeller  
Norway

1

**OTHER DISTRIBUTION**

To be determined by the project office

9

**TOTAL 81**